
# NIC Symposium 2014

12 – 13 February 2014
Forschungszentrum Jülich, Germany

**Programme**

**Bus Schedule**

**Poster Abstracts**

**Participants**

# Programme

## Wednesday, 12 February 2014

| | |
|---|---|
| 8:30 | Transfer from Jülich |
| 8:45 | Registration |
| 9:15 | **Welcome Address** by A. Bachem, Chairman of the Board of Directors, Forschungszentrum Jülich |
| 9:30 | G. Münster, Vice Chairman of the NIC Scientific Council<br>**Introduction to the NIC Symposium** |
| 9:45 | K. Kremer, MPI für Polymerforschung, Mainz<br>**Computer Simulations of Soft Matter at HLRZ/NIC - A Success Story** |
| 10:30 | Coffee |
| 11:00 | Th. Lippert, Forschungszentrum Jülich<br>**Paving the Road towards Pre-Exascale Supercomputing** |
| 11:45 | St. Gottlöber, Leibniz-Institut für Astrophysik, Potsdam<br>**A Coherent Hubble Volume Simulation for All-Sky ISW Predictions and Large Scale Surveys** |
| 12:30 | Lunch |
| 14:00 | M. Hohenadler, Universität Würzburg<br>**Numerical Simulations of Correlated Quantum Matter** |
| 14:45 | K. Michielsen, Forschungszentrum Jülich<br>**Simulation of Equilibration and Decoherence in Quantum Systems** |
| 15:30 | Coffee |
| 16:00 | G. Münster, Universität Münster<br>**Numerical Simulation of Supersymmetric Yang-Mills Theory** |
| 16:45 | K. Szabo, Universität Wuppertal<br>**Isospin Splittings in the Light Baryon Octet from Lattice QCD+QED at the Physical Mass Point** |
| 17:30 | **Poster Session and Reception** |
| 19:00 | Transfer to Jülich |

## Thursday, 13 February 2014

8:30 Transfer from Jülich

9:00 J. Dąbrowski, IHP, Frankfurt/Oder
***Ab initio* Modelling of Growth of Graphene for Silicon-Compatible Electronics**

9:45 D. Muñoz-Santiburcio, Ruhr-Universität Bochum
**Prebiotic Chemistry on Blue Gene Platforms**

10:30 Coffee

11:00 M. Müller, Universität Göttingen
**Directing the Assembly of Block Copolymers: A Single-Chain-in-Mean-Field Simulation Study**

11:45 H. Gohlke, Universität Düsseldorf
**Interplay of Structure, Energetics, and Dynamics for Antibiotics Binding to and Control of Gene Expression by RNA**

12:30 Lunch

14:00 A. Kurzmann, Karlsruher Institut für Technologie
**3D Acoustic Full Waveform Tomography**

14:45 G. Lehmann, Universität Düsseldorf
**Laser-Pulse Amplification by Raman and Brillouin Scattering Towards Multipetawatt Level**

15:30 Coffee

16:00 Th. Boeck, TU Ilmenau
**Wall-Bounded Liquid-Metal Flows in Magnetic Fields - Flow Structures, Turbulence and the Transition Problem**

16:45 M. Bolten, Universität Wuppertal
**Multigrid Methods for Structured Matrices on Large-Scale Supercomputers**

17:45 Transfers to Jülich and to Düren Train Station

# Bus Schedule

Bus is free of charge for participants.

| Date | Departure Time | Meeting Point | Destination |
|---|---|---|---|
| 12 February | 08:30 | Bus stop "Walramplatz" | Research Centre Jülich, Auditorium |
| | 08:35 | Bus stop "Neues Rathaus" | |
| | 19:00 | Research Centre Jülich, Auditorium | Hotels in Jülich |
| 13 February | 08:30 | Bus stop "Walramplatz" | Research Centre Jülich, Auditorium |
| | 08:35 | Bus stop "Neues Rathaus" | |
| | 17:45 | Research Centre Jülich, Auditorium | Hotels in Jülich |
| | | | Düren Train Station |

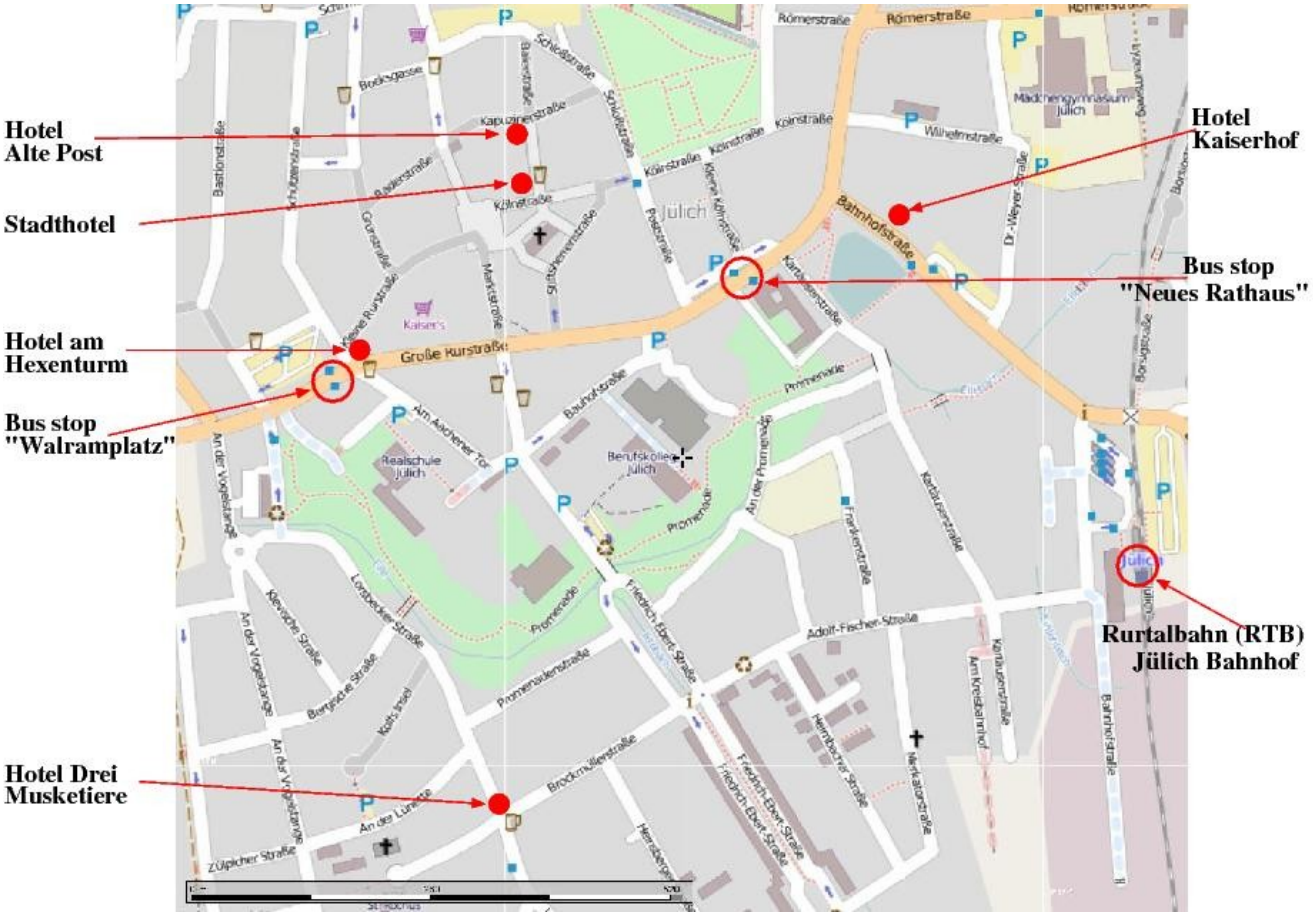

# Poster Abstracts

The number in brackets in front of the title is the number of the movable wall where to place the poster for the poster session.

## Earth and Environment

### [1] Efficient Parallel Methods for 3D-Applications in Atmospheric Sciences

*M. Baumann, **T. Beck**, S. Gawlok, V. Heuveline, S. Ronnås*

In the last decades, numerical simulation has become an indispensable tool for the atmospheric sciences. In particular, weather forecasting and climate prediction depend on the possibility of performing accurate and efficient computations. Typically, the phenomena considered in such models are influenced by processes on a wide range of spatial and temporal scales. For instance, a tropical cyclone is embedded in a large scale atmospheric flow with a length scale on the order of 10000 km, but its core spans a range of only a few kilometers.
The consideration of such processes in numerical computational fluid dynamics models is a challenging and computationally expensive task. Due to their multi-scale nature, high resolution in the discretization is required, which leads to very large systems of equations. Furthermore, their conditioning is worsened by increasing resolution, which in turn results in slow convergence. This is especially true for three-dimensional models.
The size of the system of equations can be reduced through the use of adaptive methods, that aim at a local adaptation of the discretization in space and/or time. To fully incorporate multi-scale properties in the discretization, it is often sufficient to apply high resolution only in areas with small-scale features and to keep a coarser resolution elsewhere. In this way, the total number of unknowns can be reduced remarkably. Still, for solving realistic scenarios the size of the systems remains large enough to make the use of parallel computers indispensable. Hence, solution methods that remain efficient even when scaled to a large number of processors must be applied. A central issue is to find parallel preconditioning methods that effectively handle the multi-scale nature of the equations, while not deteriorating as the number of processors grows. Several approaches have been investigated, including domain decomposition and approximate block factorizations. Experience has shown that there is no universal solution to attain good performance; rather the choice of methods must take into account the specific properties of each application.
In the project “Adaptivity for meteorological 3D-applications” (hka14), we investigate a three-dimensional scenario of two interacting tropical cyclones. Our aim is to optimize both the temporal and spatial mesh with respect to a user-defined functional. To validate the three-dimensional simulation method, we consider a baroclinic wavetank, a laboratory experiment, that can be used as an idealized representation of the atmospheric large scale flow. In this setting, we can compare the numerical results with real experimental data, which is generally very difficult in atmospheric sciences. In the related project “Scalable Preconditioners with Hybrid Parallelization for Computational Fluid Dynamics” (hka15), we compare the performance and scalability of different preconditioners for a three-dimensional fluid flow benchmark application. The simulations in both projects are based on the open-source parallel finite element software HiFlow³. Our poster presents the results achieved so far from both projects.

**[2] Direct Numerical Simulation of Turbulent Mixing in the Planetary Boundary Layer**

***J. P. Mellado**, C. Ansorge*

Small-scale turbulence determines some relevant properties of the planetary boundary layer, like the way it grows into the upper troposphere or the details of the near-surface region. However, there are still significant inaccuracies in the parametrization of these small-scale processes in weather and climate models. These inaccuracies are often due to a lack of understanding of the processes themselves, and not only to the way we represent their effect on a larger scale. We use high-performance computing and direct numerical simulation to gain new insight into long-standing, critical aspects of turbulent mixing in the planetary boundary layer and to reduce thereby those inaccuracies. This poster considers two problems: *(i)* the stratocumulus top, in particular, the turbulent mixing and the role of local phenomena therein, like evaporative cooling or radiative processes, and *(ii)* the stable boundary layer, the mechanisms of reduction, intermittency and collapse of turbulence in it.
Turbulent mixing and the role of evaporative cooling in the stratocumulus-top dynamics has remained controversial during the recent decades: though it is difficult to study such small-scale processes, of the order of tens of meters or less, they are important on a large scale because the horizontal extension of the cloud deck is large enough to affect the earth's radiative balance. Recent work has demonstrated that, in contrast to previous postulates, buoyancy reversal caused by evaporative cooling is not a sufficient condition to break up the cloud: turbulence is indeed enhanced, but very mildly. To become relevant, evaporative cooling requires the interaction with other local mechanisms of turbulence generation. We have extended that work to explain how, and under which conditions, mixing enhancement by wind shear can render evaporative cooling comparable to shear-free radiative cooling.
The motivation to investigate the stable boundary layer is that most atmospheric models rely on flux parametrizations providing the lower boundary conditions and vertical diffusivities in the vicinity of the lower boundary, and the correct prescription of those properties remains a challenge, in particular under very stable stratification. We use here Ekman flow with an appropriate Dirichlet boundary condition to study turbulence in a prototype stable boundary layer. The stratification is varied in terms of one single parameter (a bulk Richardson number) such that we can reproduce weakly, intermediately and strongly stratified turbulence. We find global intermittency, despite the absence of external forcing other than an external pressure gradient which drives the Ekman boundary layer. The globally intermittent flow is studied in terms of the mean wind, the flow enstrophy, and kinetic energy of the mean and perturbations.

**[3] Towards Convection Permitting Regional Climate Simulations in the Alpine Region: Experiences from the Wegener Center**

***H. Truhetz**, A. Prein*

Since their introduction in the late 1980s, regional climate models (RCMs) are widely applied in climate research and climate change impact studies. Nowadays, they are used to provide climate change data on model grids with ~10 km grid spacing or above, e.g. within EURO-CORDEX (www.euro-cordex.net), the European branch of the Coordinated Downscaling Experiment of the World Climate Research Programme (WCRP). However, a further increase of the resolution towards convection permitting/resolving scales (horizontal grid spacing <4 km) is not straightforward: (1) RCMs need reconsideration, because relevant processes (e.g. deep convection) on former unresolved (parameterised) scales become resolved, (2) highly resolved land surface information is necessary as input for the lower boundary conditions, and (3) the demand of computational resources increases exponentially when grid spacing is reduced. Further difficulties are lying in model evaluation: (1) highly resolved observational data for model evaluation only exist in exceptional cases and (2) advanced statistical methods have to be applied to evaluate highly resolved daily or sub-daily spatial structures of e.g.

precipitation to account for temporal and spatial displacements.
The poster presents latest results from the Wegener Center on its way establishing convection permitting climate simulations (CPSCs). Within the framework of the research project “Non-Hydrostatic Climate Modelling, Part I (NHCM-1)”, funded by the Austrian Science Fund (FWF) (project number P19619-N10) fuzzy and object oriented evaluation techniques (FSS, SAL) adopted from numerical weather prediction (NWP) were applied on a small multi RCM ensemble (COSMO-CLM, MM5, and WRF) in order to investigate added value of CPCSs in the Eastern Alpine region. For that purpose, data from the highly resolved (1 km grid spacing) now casting system INCA of the Austrian Central Institute for Meteorology and Geodynamics (ZAMG) was used as reference data. The poster summarises important results from that work and provides an outlook on the next steps that are taken in the follow-up project NHCM-2 (www.nhcm-2.eu), funded by FWF (project number P24758-N29).

**[4] First-Principles View on Element and Isotope Cycles in the Earth's Interior**

***S. Jahn**, V. Haigis, P. M. Kowalski, D. Künzel, G. Spiekermann, J. Wagner*

Throughout Earth's history, chemical elements and their isotopes have been continuously recycled and redistributed. The related chemical and transport processes are especially efficient in the presence of melts or fluids. We use molecular dynamics simulation techniques to investigate the thermodynamics of fluid- or melt-rock interactions and develop predictive models of equilibrium trace element partitioning and stable isotope fractionation between coexisting phases. This approach does not only require an accurate description of atomic interactions but also reliable structure models for the constituting minerals as well as for the melt or fluid phase at relevant pressure and temperature conditions of the Earth's interior. On top of classical and *ab initio* molecular dynamics simulations used for a statistical sampling of fluid and melt structures we develop and employ advanced numerical methods to validate our models against experiments and to derive element and isotope partition coefficients.

**[5] Numerical Modelling of Lithospheric and Crustal-Scale Deformation on Geological Timescales**

***B. Kaus**, T. Baumann, A. Popov , E. Boutonnet, N. Fernandez, A. Püsök, D. May, M. Collignon*

Computational geodynamics uses numerical modelling to understand fundamental geoscientific questions such as: Why do we have plate tectonics on Earth and not on other planets? How did mountain belts such as the Alps and the Himalaya form and what is the role of erosion in this? At the same time, computational geodynamics also addresses more practical questions related to the evolution of so-called fold- and thrust-belts and salt diapirs, which are closely linked with the majority of the world’s oil reservoirs.
We have developed a 3D numerical code, which simulate the deformation of the lithosphere and its interactions with the underlying mantle and surface. The code solves the incompressible, variable viscosity Stokes equations using a conservative finite difference formulation in combination with a marker and cell method, to simulate large strains.
In this project, we employ the code to study the dynamics of fold and thrust belts, the formation of salt domes, continental collision in the Himalaya on a million year timescale and the structure and dynamics of the present-day alps. We have also coupled it with a Monte-Carlo inversion scheme in order to determine optimal material parameters of the lithosphere from geophysical surface observations.

**[6] Multiphase Chemistry in the Earth System - from Chemistry to Climate**

***H. Tost***

Chemical processes in the atmospheric system can have a substantial influence on the climate system. In this study, the influence of chemical processing of natural and anthropogenic compounds in clouds and the treatement of chemical conversions dissolved in the aqueous phase are analysed. Furthermore, the effect of natural emissions of nitrogen oxides by lightning on the climate system is investigated. Originating from the NOx emissions, nitrate aerosols can be formed. Both processes can alter radiative transfer in the atmosphere due to light scattering (direct aerosol effects) and can contribute to the cloud condensation nuclei budget, but also modify other aerosol particles to be inefficient ice nuclei, thus influencing the radiative properties of clouds (indirect aerosol effects). Global model simulation results are presented, which shed light onto the involved processes from emission and transport to aerosol formation and the interactions with radiative transfer in the atmosphere.

**[7] Enabling Climate Simulation at Extreme Scale: Performance Analysis and Modeling**

***M. Lücke****, A. Calotoiu, F. Wolf*

Many parallel applications suffer from latent performance limitations that may prevent them from scaling to larger machine sizes. Especially climate codes would benefit from improved parallel efficiency and scalability, because their simulations often run for months and higher core counts would allow for higher resolution and enhanced physics. Considering the code size and intricacy of such community codes, scalability bottlenecks, e.g., inefficient data structures, algorithms or insufficient load balancing, are very hard to detect and even harder to remediate. Within the ECS project, we develop methods and tools that support application developers in uncovering scalability problems and assist them in optimizing load balance for more efficient resource utilization.
In a first approach we used well-established performance analysis tools, in particular Scalasca, to study the performance of the Community Earth System Model (CESM) and its specific models. We were able to trace poor scalability of some communication routines within the ocean and sea ice model back to load imbalance in associated computation phases. Although load balance is crucial for efficient resource utilization, it is often very difficult for application developers to find a suitable load-balancing strategy that fits their specific problem. In addition, implementation and test of different load balancing strategies is usually not possible without major code surgery. We implemented a load-balancing simulator as a software engineering tool that enables developers to easily test and experiment with different load-balancing strategies based on an abstract description of their application. It enables scientific application developers to study their application's behavior and the associated potential performance yield without cumbersome analytical comparison or time consuming modifications of the real code and subsequent tests. We initially used the simulator to compare the load-balancing strategy of a sea ice simulation to an alternative algorithm and estimated a speedup of 2.7 due to the reconfiguration. A study involving a broader set of execution configurations is in progress.
Besides load imbalance, applications may entail other latent performance limitations, which would show only on larger scale. An established method of foreseeing such problems is performance modeling, however the creation of performance models is laborious and rarely possible for an entire application. A performance model describes the runtime or other performance properties in a mathematical representation that enables analysis and extrapolation of the property for different parameters, such as core count. Using automated performance modeling we can easily identify those parts that will reduce performance at larger core counts. We have studied HOMME, the dynamical core of the Community

Atmospheric Model (CESM-CAM) and found two scalability issues, one of which was previously unknown.

**[8] Porting and Scaling of the Fully Coupled Terrestrial Systems Modelling Platform (TerrSysMP) on IBM BG/Q JUQUEEN**

***K. Goergen**, S. Kollet, F. Gasper, P. Shrestha, M. Sulis, J. Rihani, C. Simmer, H. Vereecken*

Terrestrial systems research is dealing with complex interactions between various sub-systems of the geo-ecosystem on a multitude of space and time scales. In addition to natural variability, anthropogenic system changes modify land surface and ecosystem processes resulting in various socio-economic impacts. The differentiation and quantification of natural and anthropogenically induced variability of the full hydrologic cycle at climate time scales constitutes a grand challenge in Earth system science. Tackling this challenge requires integrated multi-physics modelling platforms, such as the Terrestrial Systems Modelling Platform (TerrSysMP), that simulate the terrestrial hydrologic, energy and biogeochemical cycles from deeper aquifers across the land surface to the top of the atmosphere. Based on existing component models, TerrSysMP has been developed in recent years in the Transregional Collaborative Research Centre 32. During 2013, it was ported and optimized to run on the IBM BG/Q system JUQUEEN at the Jülich Supercomputing Centre (JSC). Here we present our experience from coupling, application tuning, parallel scaling and performance monitoring of TerrSysMP on JUQUEEN.

In TerrSysMP, the physics-based models COSMO (atmosphere), CLM (land surface) and ParFlow (groundwater and surface water flow) are coupled through the external coupler OASIS3 and OASIS-MCT. The platform is highly portable and may be used on small commodity clusters as well as massively parallel HPC systems. It is used from regional watersheds up to Pan-European model domains in real-data and idealized conceptual “virtual reality” studies at spatial resolutions down to sub-km scales. In these simulations variances in water, energy and biogeochemical fluxes and states are characterized over multiple orders of magnitude, considerably advancing our understanding of non-linear feedbacks in the terrestrial system.

After the initial porting, a systematic performance analysis including profiling and tracing was done to uncover parallel inefficiencies, better understand runtime behaviour and identify optimum model settings using the Scalasca performance optimisation tool. Substantial speedups could be obtained through compiler optimizations and optimum model settings. Because independent executables are coupled, a Multiple Program Multiple Data (MPMD) execution model is needed to run TerrSysMP. In this setup, profiling and tracing data was utilized to identify optimum (static) resource allocations amongst the component models for each (new) model setup, in search of the most suitable load balancing. In order to run large model domains and use all CPU cores of the low-RAM JUQUEEN nodes (1 GB / CPU-core), a refactoring of the coupling scheme from an external executable (OASIS3) to an integrated library (OASIS3-MCT) was necessary. Starting initially with 512 MPI tasks in February 2013, TerrSysMP can now efficiently be applied with more than 32k processes.

# Computational Soft Matter Science

### [9] Polymer Dynamics in Confinement: MD Simulations of 1,4-Polybutadiene at a Graphite Interface

***M. Solar**, L. Yelash, P. Virnau, K. Binder, W. Paul*

Polymer dynamics in confinement is both of fundamental interest concerning our understanding of the glass transition, as well as of high technological importance for the performance of composite materials. The results here presented are concerned with atomistic MD simulations of a chemically realistic model of a 1,4-polybutadiene melt (55% trans and 45% cis content, randomly dispersed) confined between two walls of graphite. The focus of our study is to investigate the effects of confinement on the chain dynamics in the melt and to reveal to what extent the walls are influencing structure and dynamics of the melt. The physical properties here investigated are concerned with the structure and the topology of the chains in the confined melt and also with dynamic relaxation of various chain motions. The results presented are key to a better understanding of the glass transition process in a confined polymer system.

### [10] Scaling Properties of a Parallel Implementation of the Multicanonical Algorithm

*J. Zierenberg, **M. Marenz**, W. Janke*

The multicanonical method has been proven powerful for statistical investigations of lattice and off-lattice systems throughout the last two decades. We discuss an intuitive but very efficient parallel implementation of this algorithm and analyze its scaling properties for discrete energy systems, namely the Ising model and the *8*-state Potts model. The simple parallelization relies on independent equilibrium simulations in each iteration with identical multicanonical weights, merging their statistics in order to obtain estimates for the successive weights. With good care, this allows faster investigations of large systems, because it distributes the time-consuming weight-iteration procedure and allows parallel production runs. We show that the parallel implementation scales very well for the simple Ising model, while the performance of the *8*-state Potts model, which exhibits a first-order phase transition, is limited due to emerging barriers and the resulting large integrated autocorrelation times. The quality of estimates in parallel production runs remains of the same order at same statistical cost.

### [11] Effect of Bending Stiffness on a Homopolymer inside a Spherical Cage

***M. Marenz**, W. Janke*

We study the change of the pseudo phase transition of a simple homopolymer inside a spherical confinement. Of particular interest is the shift of the collapse and freezing transitions with shrinking radius of the sphere. The polymer is a simple bead-stick model, where the distance between neighboring monomers is fixed, between three monomers in a row acts a bending potential and all non neighboring monomers interact via a Lennard-Jones potential. We use modern Monte Carlo methods to investigate the phase space of this model. Most of the results are obtained by parallel tempering simulations followed by a multi-histogram reweighting method combining a direct and a recursive procedure. To crosscheck our results, especially near the pseudo phase transition, we used a parallelized kind of the multicanonical simulation. To characterize the pseudo phase transition we analyse fluctuations of energetic and conformational observables. As zero order case the spherical cage is modeled only as a

geometrical constraint without any interaction with the polymer. In further simulations we switched on a interaction between the polymer and the surface of the sphere and looked for effects induced by this interaction.

### [12] Effect of Chain Stiffness on the Adsorption Transition of Polymers

***H.-P. Hsu**, K. Binder*

Polymers grafted with one chain end to an impenetrable flat hard wall which attracts the monomers with a short range adsorption potential (of strength ε) are studied by large scale Monte Carlo simulations, using the Pruned-Enriched Rosenbluth method (PERM). Chain lengths up to N=25600 steps are considered, and the intrinsic flexibility of the chain is varied via an energy penalty for nonzero bond angles, $\varepsilon_b$. Choosing $q_b = \exp(-\varepsilon_b/k_BT)$ in the range from $q_b=1$ (fully flexible chains) to $q_b=0.005$ (rather stiff chains with a persistence length of about $\ell_p=52$ lattice spacings) [1,2], the adsorption transition is found to vary from about $\varepsilon/k_BT_c\approx0.286$ to $\varepsilon/k_BT_c\approx0.011$, confirming the theoretical expectation that $\varepsilon/k_BT_c \mu 1/\ell_p$ for large $\ell_p$. The simulation data are compatible with a continuous adsorption transition for all finite values of $\ell_p$, while in the rigid rod limit ($\ell_p\rightarrow\infty$) a first order transition seems to emerge. Scaling predictions and blob concepts on the structure of weakly adsorbed semiflexible polymers absorbed at interfaces are briefly discussed [3].

References:
[1] H.-P. Hsu, W. Paul, and K. Binder, EPL **92**, 28003 (2010).
[2] H.-P. Hsu, W. Paul, and K. Binder, EPL **95**, 68004 (2011).
[3] H.-P. Hsu and K. Binder, Macromolecules **46**, 2496 (2013).

### [13] Pulling Single Adsorbed Bottle-Brush Polymers off a Flat Surface: A Monte Carlo Simulation

*H.-P. Hsu, K. Binder, **W. Paul***

Force versus extension behaviour of flexible chains and semiflexible bottle-brush polymers adsorbed from a good solvent on a planar substrate is studied by Monte Carlo simulation of the bond fluctuation model. The properties of the polymers (fraction of adsorbed monomers, height of the free end of the macromolecule above the surface, gyration radius components parallel and perpendicular to the surface, etc.) are studied in full thermal equilibrium as well as out of equilibrium, varying the pulling speed over three orders of magnitude. The equilibrium extension vs. force curve reveals that the transition force (where force-induced desorption occurs) increases with increasing side chain length N of the bottle brushes, while further extension is almost independent of N, and can be described by a model due to Odijk, in agreement with a recent experiment.

### [14] End-Functionalized Semiflexible Polymer Suspensions at Equilibrium and under Shear Flow

*J. S. Myung, **F. Taslimi**, R. G. Winkler, G. Gompper*

Functionalized polymers are able to self-organize into complex structures covering a broad-range of length scales and thus provide the building blocks for novel complex materials. Examples are suspensions of low-density end-functionalized rodlike polymers, which exhibit a novel scaffold-like structure above a certain adhesive strength. Naturally, this structure affects

or even controls the rheological behavior of these systems. We investigate the equilibrium and non-equilibrium behavior of such end-functionalized semiflexible polymer suspensions by using mesoscale hydrodynamic simulations. The hybrid simulation approach combines the multiparticle collision dynamics (MPC) method for the fluid, thereby accounting for hydrodynamic interactions, with molecular dynamics (MD) simulations for the semiflexible polymers. Scaffold-like network structures of the polymers are observed in equilibrium, which are governed by the polymer flexibility and end-attraction strength. The stiffness-dependent structural properties are discussed for various polymer concentrations and adhesive strengths. In addition, we investigate the flow behavior of the polymer network under shear and analysis the non-equilibrium structural and rheological properties. Our studies provide a deeper understanding of the equilibrium and non-equilibrium dynamical behavior of the complex structures.

# Computational Biology and Biophysics

### [15] Water@surface: Vibrational Signature of Water Molecules in Asymmetric Hydrogen Bonding Environments

***C. Zhang**, T. D. Kühne*

The O-H stretching vibrational modes of water molecules are sensitive to their local environments. Here, we combine the strength of DFT-based MD, effective normal modes analysis (ENM) and novel energy decomposition analysis (ALMO-EDA) to investigate the hydrogen bonding network in liquid water and water interface in biological environments. As an important milestone, we established the correlation between the local hydrogen bonding asymmetry and novel vibrational descriptors in liquid water, which is generally applicable for any reasonably accurate model of water and useful for interpreting experimental Raman, infrared and sum-frequency generation (SFG) spectra of interfacial water molecules. Subsequently, we extend our methodologies to investigate the water molecules at the surface of an antifreeze protein.

### [16] Molecular Insights into Binding of Oxazolidinone Antibiotics to the Large Ribosomal Subunit

*J. S. Saini, N. Homeyer, S. Fulle, **H. Gohlke***

The ribosome is a ribozyme that catalyses the mRNA-directed protein synthesis [1]. Prokaryotic ribosomes are composed of two unequal subunits (30S and 50S). The subunits contain several important functional sites that act as potential antibiotic targets, one of which is the peptidyl transferase center (PTC) located in the large ribosomal subunit. Although there are many antibiotics available already, the ever increasing emergence of multi-drug-resistant bacteria stresses the need to identify new antibiotics. Oxazolidinones represent one of only two new chemical classes of antibiotics that have been introduced in the clinics over the past 40 years. Linezolid, the only member of this class approved by the FDA, binds to the PTC and shows excellent activity against major Gram-positive bacteria [2]. The available co-crystal structures of linezolid with the large ribosomal subunit of Deinococcus radiodurans (D50S) [3] and Haloarcula marismortui (H50S) [4] provide static views of the binding processes but do not reveal the dynamics involved with antibiotics binding.
In order to provide a better understanding of binding determinants and factors that give rise to selectivity or the development of resistance, we have performed for the first time molecular dynamics (MD) simulations in combination with MM-PBSA [5] free energy calculations of linezolid and two other oxazolidinone derivatives, radezolid and rivaroxaban, bound to D50S and H50S. On an atomic level, the analyses reveal an intricate interplay of structural, energetic, and dynamic determinants of the binding and species-selectivity of oxazolidinone antibiotics. A structural decomposition of free energy components identifies influences that originate from first and second shell nucleotides of the binding sites and lead to contributions from interaction energies, solvation, and entropic factors [6]. Moreover, double mutations 10 Å away from the binding site synergistically contribute to linezolid resistance due to the percolation of effects from interaction changes through the ribosomal structure. These findings suggest that analyzing binding of antibiotics to targets as complex as the ribosome solely based on structural information and qualitative arguments on interactions may not reach far enough. The computational analyses presented here should be of sufficient accuracy to fill this gap.

References:
[1] T. A. Steitz and P. B. Moore, Science (2003) 8, 411-418.

[2] K. L. Leach et. al, Ann N Y Acad Sci (2011) 1222, 49-54.
[3] D. N. Wilson et. al, Proc. Natl. Acad. Sci. (2008) 105, 13339–13344.
[4] J. A. Ippolito et. al, J. Med. Chem. (2008) 51, 3353–3356.
[5] H. Gohlke, D. A. Case, J. Comput. Chem. (2004) 25, 238-250.
[6] J. S. Saini et. al, Biol. Chem. (2013), 394, 1529-1541.

**[17] How Tertiary Interactions between the L2 and L3 Loops Affect the Dynamics of the Distant Ligand Binding Site in the Guanine Sensing Riboswitch**

***C. A. Hanke**, H. Gohlke*

Riboswitches are gene regulatory RNA elements that control bacterial gene expression on the transcriptional or the translational level upon binding of ligand molecules. They consist of two domains: the aptamer domain, which is able to bind a ligand with high specificity, and the expression platform, which undergoes a conformational change upon binding of the ligand to the aptamer domain. In transcriptionally acting riboswitches, this conformational change of the expression platform leads to the formation or disintegration of an intrinsic transcription terminator loop and thus to switching gene expression off or on. Since transcriptional gene regulation by riboswitches has to happen in a narrow time window during transcription, detailed knowledge about the unbound state of the riboswitch is crucial for understanding the regulation decision. Insights into the bound state of purine binding riboswitches, such as the guanine and adenine sensing riboswitches, are available from crystal structures and other experimental investigations. However, atomic level details of the unbound state and its dynamics are still unknown.
In order to investigate how tertiary interactions in the L2/L3 loop region of the guanine sensing riboswitch aptamer domain (Gsw) affect the aptamer domain's ability to bind ligands, we performed molecular dynamics simulations of wildtype Gsw and a G37A/C61U mutant of in total 9 μs length. The simulations reveal a dynamic coupling between the loop region and the distant ligand binding site suggesting that there exists a complex pathway for the transmission of stability information through the aptamer domain. This finding may have important implications for understanding how Gsw functions at a molecular level.

**[18] The Ripple Effect: Connecting a Single Mutation in Integrin αIIbβ3 with an Increased Tendency for Myocardial Infarction**

***G. Pagani**, N. Homeyer, V. R. Stoldt, R. E. Scharf, H. Gohlke*

The megakaryocyte/platelet-specific integrin αIIbβ3 mediates platelet adhesion and aggregation and is essential for hemostasis but can also foster thrombus formation. The HPA-1 polymorphism of αIIbβ3 arises from a leucine-to-proline exchange at residue 33 of the mature β3 subunit resulting in HPA-1a (Leu33) or HPA-1b (Pro33) platelets [1]. Genotyping revealed that patients with coronary artery disease who carry the HPA-1b allele experience their myocardial infarction 5.2 years earlier than HPA-1a/1a patients [2]. While these observations suggest that HPA-1b (Pro33) is a prothrombotic variant of αIIbβ3, the mechanism at an atomic level by which the mutation contributes to integrin activation has remained elusive so far. In this study, we investigated consequences of the Leu33Pro exchange on the structure and dynamics of αIIbβ3 by molecular dynamics (MD) simulations in explicit solvent of in total 500 ns length. On a global level, our simulations reveal that the Pro33 (HPA-1b) isoform of αIIbβ3 is, in line with the clinical findings, increasingly activatable. In atomic detail, our simulations indicate that in the Pro33 variant stabilizing interactions of the PSI domain, located in the head region, with the nearby EGF-I and EGF-II domains, located in the leg region of αIIbβ3, are lost allowing the protein to open and become active more rapidly. These results provide insights how a mutation at a position > 90 Å away from any

binding site in αIIbβ3 can allosterically affect the fine-tuned conformational equilibrium of the integrin. Further simulations are currently being carried out to determine the influence of the transmembrane domains of αIIbβ3 on its activation.

References:
[1] Kunicki,T.J. and Newman, P.J. The molecular immunology of human platelet proteins. Blood 1992, 80: 1386-1404.
[2] Zotz R.B., Winkelmann B.R., Müller C., Boehm B.O., Marz W., Scharf R.E. Association of polymorphisms of platelet membrane integrins αIIbβ3 (HPA-1b/PlA2) and α2β1 (a2807TT) with premature myocardial infarction. J. Thromb. Haemost. 2005, 3: 1522-93.

## [19] Anion Permeation through Excitatory Amino Acid Transporters

***J.-P. Machtens**, D. Kortzak , C. Lansche, A. Leinenweber, P. Kilian, B. Begemann, U. Zachariae, D. Ewers, B. L. de Groot, R. Briones , C. Fahlke*

Glutamatergic synaptic transmission critically depends on excitatory amino acid transporters (EAATs) that remove released neurotransmitters from the synaptic cleft and thereby ensure low extracellular glutamate concentrations in the central nervous system. EAATs are thermodynamically coupled glutamate/$Na^+$/$H^+$/$K^+$ transporters and anion-selective channels. EAAT anion channels control neuronal excitability and synaptic communication, and their physiological importance is further corroborated by the recently identified association of altered EAAT anion conduction with neurological disorders. The five mammalian EAATs differ in their effectiveness as glutamate transporters and anion channels. However, pore properties of the known isoforms such as anion selectivity and unitary current amplitudes appear to be closely similar. Although important structural information on secondary-active glutamate transport has been resolved in recent years, the molecular mechanisms underlying anion permeation are still unknown. We here performed molecular dynamics (MD) simulations of the prokaryotic EAAT homologue $Glt_{Ph}$ to elucidate how these transporters conduct anions. Our results are validated by fluorescence quenching experiments on single-tryptophane mutants of $Glt_{Ph}$ and patch-clamp recordings of mammalian EAATs. Whereas outward- and inward-facing conformations of $Glt_{Ph}$ were found to be non-conductive in MD simulations, a voltage-dependent lateral movement of the mobile glutamate transport domain from an intermediate conformation led to the opening of an anion-selective conduction pathway. Amino acid substitutions of homologous pore-forming residues have similar effects on experimental EAAT2/EAAT4 and simulated $Glt_{Ph}$ single-channel conductances and anion/cation selectivities. Thus, the here identified anion conduction pathway appears to be conserved within the whole glutamate transporter family. Our results highlight how the glutamate transporter family accommodates an anion channel together with a transporter in one single protein.

## [20] A General Approach for the Study of Protein Dynamics Using Mesoscale Simulations

***S. Poblete**, R. G. Winkler, G. Gompper*

The dynamics of the subdomains of a protein can play a fundamental role in its functionality. Such motions can be studied by techniques like neutron spin-echo spectroscopy, which has been shown to be able to resolve the time and length scales in the study of proteins like alcohol dehydrogenase (ADH) and phosphoglycerate kinase (PGK) [1]. On the other hand, computer simulations can provide a deeper insight of the protein dynamics, and be of great help for the interpretation of the experimental results. The computational modelling of dynamics on such systems requires the proper introduction of solvent-mediated interactions.

We present the results for the models of several proteins where the solvent has been simulated under the Multiparticle Collision Dynamics [2,3] approach, a particle-based simulation method able to capture the hydrodynamic interactions between the domains of our models.
We begin with a simple geometrical model for the MerA protein [4], and fundamental enzyme for the resistance to toxic mercury compunds in certain bacteria, composed of a core and two terminals [5]. We continue with a general procedure for obtaining diffusion properties of globular proteins of arbitrary shape, to conclude with the analysis of a flexible model of PGK [6]. The latter has been constructed according to data obtained from FRET measurements [7]. All these models stress the power and simplicity of these coarse-grained approaches.

References:
[1] R. Inoue et al., Biophys J. 99, 2309 (2010);R. Biehl et al., Soft Matter 7, 1299 (2011) .
[2] A. Malevanets and R. Kapral, J. Chem. Phys. 110, 8605 (1999).
[3] G. Gompper et al., Adv. Polym. Sci. 221, 1 (2009).
[4] T. Barkay et al., FEMS Microbiology Reviews 27, 335 (2003).
[5] H. Liang et al., submitted.
[6] S. Poblete et al., in preparation.
[7] M. Gabba et al., in preparation.

**[21] *Ab Initio* Monte Carlo Folding of the Designed 92-Residue Alpha+Beta Protein TOP7**

***O. Zimmermann**, J. H. Meinke, S. Mohanty*

Despite recent progress in both algorithms and available computer power there are only few reports of unbiased folding simulations for non-trivial proteins. We have recently performed High Performance Monte Carlo simulations using ProFASi and, starting from random conformations, could reproducibly simulate folding of TOP7, an ultra-stable designed protein. With 92 residues this is the largest and by far most complex protein for which *ab initio* folding simulation has been reported to date. Due to its extreme stability and its complex folding landscape special analysis methods are required to derive its free energy landscape of folding at relevant temperatures. Our simulations are in line with the experimental results regarding stability and folding properties of TOP7 and mark significant progress in the field.

**[22] Structural Prediction of the Disordered N-Terminal Domain of the Prion Protein: Role of Prion Disease-Linked Mutations**

***X. Cong**, N. Casiraghi, G. Rossetti, S. Mohanty, G. Giachin, G. Legname, P. Carloni*

The cellular form of the prion protein (PrP) features a disordered N-terminal domain (N-term) and a folded globular domain (GD). The N-term has been suggested to be a broad-spectrum molecular sensor that is involved in the function of PrP and in the pathology of prion diseases (Beland and Roucou 2012). However, the lack of structural description of the N-term has long hampered the attempts to understand the role of the N-term as well as that of the pathogenic mutations (PMs) in this domain that can cause inherited prion diseases. In a recently published work (Cong, Casiraghi et al. 2013), we predicted the conformational ensemble of the N-term in mouse (Mo) PrP (N-term_MoPrP) and using replica-exchange (RE) Monte Carlo (MC) simulations (Irback and Mohanty 2006) based on an implicit-solvent all-atom potential implemented in PROFASI (Irback and Mohanty 2006). N-term_MoPrP features a large ensemble of conformations containing transient secondary structures, rather than completely disordered ones (Cong, Casiraghi et al. 2013). These results are consistent with several sets

of experimental data. Moreover, we found the PMs in the N-term did not remarkably affect the conformational ensemble of N-term_MoPrP. Our findings suggest that the PMs in the N-term may cause prion diseases by altering the protein's interactions with cellular partners instead of by destabilizing the protein's native fold. Our further investigations found that the N-term of human PrP features nearly identical conformational ensemble to that of N-term_MoPrP, which indicates that MoPrP is a good model for studying human prion diseases.

References:

Beland, M. and X. Roucou (2012). "The prion protein unstructured N-terminal region is a broad-spectrum molecular sensor with diverse and contrasting potential functions." Journal of Neurochemistry 120(6): 853-868.

Cong, X., N. Casiraghi, et al. (2013). "Role of Prion Disease-Linked Mutations in the Intrinsically Disordered N-Terminal Domain of the Prion Protein." Journal of Chemical Theory and Computation 9(11): 5158-5167.

Irback, A. and S. Mohanty (2006). "PROFASI: A Monte Carlo simulation package for protein folding and aggregation." Journal of Computational Chemistry 27(13): 1548-1555.

**[23] Molecular Simulation-Based Structural Prediction of Protein Complexes in Mass Spectrometry: The Human Insulin Dimer**

***J. Li**, G. Rossetti, J. Dreyer, S. Raugei, E. Ippoliti, B. Lüscher, P. Carloni*

Protein electrospray ionization (ESI) mass spectrometry (MS)-based techniques are widely used to provide insights in structural proteomics under the debated assumption that non-covalent protein complexes being transferred into the gas phase preserve basically the same intermolecular interactions as in solution [1,2]. Here we investigate the applicability of this assumption by extending our in-house molecular simulation protocol [3] for single proteins to protein complexes. We apply our protocol to the human insulin dimer (hIns2) as a test case. Our calculations were validated by the predictions of the mean charge and the collision cross section (CCS) [4] measured in ESI-MS experiments. Long time-scale molecular dynamics simulations were carried out to derive global and local conformational deviations between the structures in gas phase and aqueous solution. Our current work demonstrates that computational approaches such as ours or those by other groups [5-7] may be instrumental to understand how desolvation affects the structure and stability of other protein complexes and may allow to establish whether the present findings can be generalized. This type of calculations may be of help for the development of efficient strategies to optimize experimental factors for control of gaseous protein ion structure in ESI-MS experiments.

References:
[1] Brady JJ, et al. (2011) Proc Natl Acad Sci U S A 108, 12217-12222.
[2] Breuker K, Mclafferty FW (2008) Proc Natl Acad Sci U S A 105, 18145-18152.
[3] Marchese R, et al. (2012) J Am Soc Mass Spectrom 23, 1903-1910.
[4] Salbo R, et al. (2012) Rapid Commun Mass Spectrom 26, 1181-1193.
[5] Meyer T, et al. (2009) Structure 17, 88-95.
[6] Patriksson A, et al. (2007) Biochemistry 46, 933-945.
[7] Marklund EG, et al. (2009) Phys Chem Chem Phys 11, 8069-8078.

# Chemistry

## [24] Molecular Dynamics Simulations of Solid-Liquid Interfaces and Nanometer Sized Droplets Evaporation

***J. Zhang**, F. Leroy, F. Müller-Plathe*

Our activity on JUROPA has focused on the study of the thermodynamics of solid-liquid interfaces and on the evaporation mechanisms of nanometer sized droplets. This activity has been supported by the cluster of excellence Center of Smart Interfaces of the Technische Universität Darmstadt.
By means of the phantom-wall algorithm developed by us to determine solid-liquid interfacial tensions, we have shown how classical MD simulations may help to develop a microscopic understanding of what drives the wetting behavior of water on flat and rough non-polar hydrophobic substrates. We showed that superficial defects on moderately hydrophobic surfaces enhance the hydrophobic nature of these surfaces [1]. We also showed that continuum thermodynamics can generally be used to predict the interfacial tension of water on non-polar surfaces with nanometer scale roughness unless water is confined in spaces of the roughness pattern narrower than three molecular diameters [2]. We developed a simple thermodynamic argumentation that we supported by simulations to show that the wetting properties of graphene and graphite are not much different due to the short range nature of the interactions between water and carbon [3].
We performed non-equilibrium MD simulations to study the evaporation of nanometer sized droplets on surfaces with chemical heterogeneity implemented in the form of a network of parallel stripes whose interaction with the fluid atoms were modified to vary the chemical contrast between them. Depending on the distance between two neighboring stripes and on the chemical contrast between these chemical domains, we observed different regimes of evaporation: (i) evaporation occurs at constant contact angle when the stripes width is smaller than 2 atomic diameter, (ii) evaporation occurs following a stick-jump-stick mechanism where the droplet evaporates while it is pinned at the boundary between two chemical domains, jumps to and sticks at another boundary when a critical value of the contact angle is reached. These simulations shed light on the effect of contact line pinning of evaporating droplets [4].
The results mentioned above were obtained by means of calculations performed on JUROPA and were published in the following references:

[1] Leroy, F. & Müller-Plathe, F., Langmuir (2011), 27, 637-345.
[2] Leroy, F. & Müller-Plathe, F., J. Chem. Theo. Comp. (2012), 8, 3724-3732.
[3] Taherian, F.; Marcon, V.; van der Vegt, N.F.A. & Leroy, F., Langmuir (2013), 29, 1457-1465.
[4] Zhang, J., Leroy, F. & Müller-Plathe, F., in preparation.

## [25] Dynamical Simulation of Electron Transfer Processes in Self-Assembled Monolayers Adsorbed at the Au(111) Surface

***P. B. Coto**, V. Prucker, Ó. Rubio-Pons, M. Bockstedte, H. Wang, M. Thoss*

Charge transfer processes in molecular systems at semiconductor or metal surfaces play a fundamental role in applications such as photonic energy conversion in organic solar cells and charge transport in molecular nanostructures. In this contribution, we present simulations of electron transfer processes in a series of self-assembled monolayers (SAM) consisting of nitrile substituted short chain alkanethiolate molecules adsorbed at the Au(111) surface. Using first principles based methods and a model electron transfer Hamiltonian [1,2] we discuss the main factors controlling, at the molecular level, the electron injection times from donor states localized at the tail group of the SAM to the conduction band of the Au(111) surface. In

particular, we analyze how the orbital symmetry of the donor state and the length of the aliphatic spacer chain of the self-assembled monolayer [3,4] affects the characteristics and dynamics of the electron injection process.

References:
[1] Kondov, I.; Cížek, M.; Benesch, C.; Wang, H.; Thoss, M. J. Phys. Chem. C 2007, 111, 11970–11981.
[2] Li, J.; Wang, H.; Persson, P.; Thoss, M. J. Chem. Phys. 2012, 137, 22A529.
[3] Blobner, F.; Coto, P. B.; Allegretti, F.; Bockstedte, M.; Rubio-Pons, O.; Wang, H.; Allara, D. L.; Zharnikov, M.; Thoss, M.; Feulner P. J. Phys. Chem. Lett. 2012, 3, 436–440.
[4] Prucker, V.; Rubio-Pons, O.; Bockstedte, M.; Wang, H.; Coto, P. B.; Thoss, M. J. Phys. Chem. C 2013, 117, 25334–25342.

## [26] A DFT Study on the Oxidative Dehydrogenation of Methanol on Ceria-Supported Vanadia Catalysts

***T. Kropp**, C. Penschke, X. Li, J. Paier, J. Sauer*

Monomeric and oligomeric vanadia clusters deposited on a ceria support are very active catalysts for the selective oxidation of methanol to formaldehyde [1]. By virtue of scanning tunneling microscopy (STM) as well as temperature-programmed desorption spectroscopy (TPD), small vanadia clusters were found to be more active than aggregations of higher nuclearity [2]. Theoretical investigations by Penschke et al. identified $VO_2$ as the most active species [3].
On the basis of a Mars-van Krevelen mechanism, different reaction pathways are proposed. The nudged elastic bands method was used to locate the transition states of the rate-determining hydrogen transfers. Based on these pathways, formaldehyde desorption temperatures were calculated. The theoretical desorption peaks are in good agreement with the experimental ones and, thus, we were able to identify the mechanism responsible for the high reactivity of monomeric $VO_2$ on the $CeO_2$(111) surface.

References:
[1] M. Baron et al., *Angew. Chem. - Int. Edit.,* **2009**, 48, 8006.
[2] M. V. Ganduglia-Pirovano et al., *J. Am. Chem. Soc.,* **2010**, 132, 2345.
[3] C. Penschke, J. Paier, and J. Sauer, *J. Phys. Chem. C,* **2012**, 117, 5274.

## [27] Ultrafast Energy Transfer to Liquid Water by Short and Intense THz Pulses

***P. K. Mishra**, O. Vendrell, R. Santra*

Liquid water is the single most important medium in which chemical and biological processes take place. Rather than acting as passive environment, the dynamics of water during chemical and biological processes play a fundamental role in the solvation and stabilization of reaction intermediate. The possibility to generate sub-ps and very intense THz pulses at free-electron lasers in full synchronization with the X-rays (XFEL) opens the possibility to time-resolved investigations of transient state of water and of molecular species dissolved in it. Liquid water has been the subject of time-resolved X-Ray spectroscopy studies at XFELs in the past. It's response to intense pulse in the infrared domain, in which mostly intramolecular vibrations are excited, and the subsequent energy dissipation processes, have been extensively studied in the past. At low frequency, THz light couples to low energy collective modes of the liquid.
Here, we investigated the response of liquid water to one-cycle, 200fs long (FWHM) THz pulses spectrally centered at about 100 $cm^{-1}$ ( 3THz). The THz pulse does not target any

particular mode of the liquid. At an intensity of about $10^{10}$ W/cm$^{-2}$, the pulse transfers energy mostly to translational modes of the water monomers along the polarization axis of the electric field. In a time-scale of 500fs to 1ps the energy redistributes to hindered rotational modes first, and to intramolecular vibrations last. This implies that the energy supplied by the THz can potentially activate chemical processes long before the large amount of energy supplied leads to volume increase and vaporization of the medium. Radial Distribution function and X-Ray diffraction pattern of water at certain time intervals are showing that water looses tetrahedral hydrogen bond structure with time due to pulse. Water reaches to a quasi-equilibrium state which is gas like very hot liquid. In this study, we have used CP2K package for *ab initio* Molecular Dynamics.

**[28] TRAVIS - Infrared and Raman Spectra From *Ab Initio* Molecular Dynamics**

***M. Brehm**, M. Thomas, B. Kirchner*

We presented TRAVIS ("TRajectory Analyzer and VISualizer"), a free program package for analyzing and visualizing Monte Carlo and molecular dynamics trajectories (see http://www.travis-analyzer.de/). The aim of TRAVIS is to collect as many analyses as possible in one program, creating a powerful tool and making it unnecessary to use many different programs for evaluating simulations. This should greatly rationalize and simplify the workflow of analyzing trajectories. TRAVIS is written in C++, open-source freeware and licensed under the terms of the GNU General Public License (GPLv3).
On this poster, we show some of the newly implemented features in TRAVIS. Two examples:

- Calculation of IR and Raman spectra from *ab initio* molecular dynamics simulations of the bulk phase, including description of anharmonicity effects.
- Construction of Voronoi cells around molecules for unbiased definition of neighborhood and investigation of molecular surfaces.

**[29] Dynamics at a Janus Interface**

***M. von Domaros***

Electric field effects on water interfacial properties abound, ranging from electrochemical cells to nanofluidic devices to membrane ion channels. On the nanoscale, spontaneous orientational polarization of water couples with field alignment, resulting in an asymmetric wetting behavior of opposing surfaces: a field-induced analogue of a chemically generated Janus interface. Using atomistic simulations, we uncover a new and significant field polarity (sign) dependence of the dipolar-orientation polarization dynamics in the hydration layer. Applying electric fields across a nanoparticle, or a nanopore, can lead to close to 2 orders of magnitude difference in response times of water polarization at opposite surfaces. Typical time scales are within the O(0.1) to O(10) picosecond regime. Temporal response to the field change also reveals strong coupling between local polarization and interfacial density relaxations, leading to a nonexponential and in some cases, nonmonotonic response. This work [1] highlights the surprisingly strong asymmetry between reorientational dynamics at surfaces with incoming and outgoing fields, which is even more pronounced than the asymmetry in static properties of a field-induced Janus interface.

References:
[1] Michael von Domaros, Dusan Bratko, Barbara Kirchner, and Alenka Luzar. Dynamics at a Janus Interface. J. Phys. Chem. C, 2013, 117, pp 4561-4567.

# Materials Science

### [30] Understanding the Phase Sequence of Fe-Pd Alloys from First-Principles Calculations and Thin Film Experiments

***M. E. Gruner**, S. Kauffmann-Weiss, L. Schulz, S. Fähler, P. Entel*

Apart from the prototypical Ni-Mn-Ga Heusler alloy, also Fe-based alloys as Fe-rich Fe-Pd exhibit significant magnetic field induced strains in moderate magnetic fields. This is bound to a slightly tetragonal fcc structure (fct) which finds no correspondence on the zero termperature energy surface which has been determined recently from first principles calculations [Phys. Rev. B 83, 214 415 (2011)]. Instead, the energy decreases rather uniformly along the Bain path towards the absolute minimum at bcc.
Magnetic excitations at elevated temperatures have decisive impact on the energy landscape suggesting that strong magnetoelastic coupling finally stabilizes the fcc austenite. Likewise changes to the energetics are encountered after alloying with a suitable third component. This aids the interpretation of the transformation behavior seen in combinatorial experiments offering further perspectives for functional design [Acta Mater. 58, 5949 (2010); J. Alloys Compd. 577, S333 (2013)].
XRD spectroscopy of thin 70at.-% Fe films epitaxially grown with a c/a=1.09, which extends the conventional Bain path far beyond fcc, and first principles modelling reveal the presence of a novel relaxation mechanism leading to a nanotwinned pattern, which consists of fct building blocks [Phys. Rev. Lett 107, 206105 (2011)]. This process owes to the extremely low formation energy of initial fct twins, which causes the autonomous evolution of a nanotwinned superstructure in the simulation cell along [110]. This corresponds to the experimentally observed soft transversal acoustic phonon in this direction, which is also a central feature of the Ni-Mn-Ga magnetic shape memory alloy.
Extending the analogy between the two systems, we finally interpret the fct phase as a metastable adaptive martensite, where the increasing twin defect energy at larger distortions prevents the relaxation to the bcc ground state.
The authors gratefully acknowledge funding by the DFG via SPP1239.

### [31] *Ab Initio* Modelling of f-Electron Materials Relevant for Nuclear Waste Management

***P. M. Kowalski**, A. B. Romero, Y. Li, G. Beridze*

Safe management of nuclear waste is a serious problem faced by society. Over the last years a significant experimental research effort has been devoted for systematic studies of methods that could be used for selective partitioning of long-lived actinides and their safe storage under repository conditions [1,2]. With the modern computational resources provided by Forschungszentrum Jülich and state-of-the-art *ab initio* methods of computational quantum chemistry we contribute to such a research by providing atomic-scale description of processes that govern interactions of f-elements with different extractants agents and candidate host materials. Density functional theory (DFT) is usually the only *ab initio* method of choice for simulation of complex fluids and solids, but it often dramatically fails to describe materials containing strongly correlated *f*-electrons. It is then a general trend to employ more reliable but much more computationally demanding methods such as hybrid DFT functionals or post Hartree-Fock methods in order to get a realistic description of the properties of lanthanide- and actinide-bearing materials [3,4]. This significantly limits the size and chemical complexity of materials that could be investigated [5]. In our contribution we show an assessment of the performance of different DFT-based computational methods in prediction of the structural and thermodynamic properties of actinide- and lanthanide-bearing materials such as simple uranium-bearing compounds and solids, monazite-type orthophosphates

($LnPO_4$) and pyrochlore ($Ln_2(Zr,Hf)_2O_7$). We show that with an appropriate choice of the computational method, the structural and thermodynamic properties of these materials can still be computed with standard DFT method or with its computationally inexpensive extensions, such as DFT+U. We demonstrate that especially the DFT+U method with Hubbard U parameter, derived *ab initio* [6], leads to significant improvement in the prediction of structural and thermodynamic parameters, such as lattice constants and reaction/formation enthalpies of the considered f-electron materials.

References:
[1] A. Wilden, *et al.*, Solvent Extr. Ion Exch. (2014), 32, 119.
[2] H. Schlenz, *et al*. *Z. Kristallogr.* (2013), 228, 113.
[3] Weng *et al., Chem. Rev.*, 2013, 113, 1063.
[4] G. A. Shamov, G. Schreckenbach, and T. N. Vo, *Chem. Eur. J.* (2007), 13, 4932.
[5] C.Hattig, "Computational Nanoscience: Do It Yourself!", S. Blügel, D. Marx, John von Neumann Institute for Computing, Jülich, *NIC Series*, (2006), 31, 245.
[6] M. Cococcioni and S. de Gironcoli , *Phys. Rev. B*, (2005), 71, 035105.

**[32] Shear Bands within Coarsened Third Body Grains Alleviate Sliding between Nanocrystalline Counter Surfaces**

***P. A. Romero**, T. T. Jaervi, N. Beckmann, M. Moseler*

Tribological shearing of polycrystalline metallic surfaces typically leads to grain refinement near the sliding interface. Therefore, one might expect this behavior to persist as the grain size is reduced to a few nanometers until an amorphous phase is established. Here, however, we show that for highly pure nanocrystalline counter bodies with grain level surface roughness; grain growth and cold welding is the preferred atomic structure evolution at the sliding interface as this leads to more deformable third body layers. Through large scale (spatial and temporal) atomistic simulations, we show that in the case of nanocrystalline iron (with grain size ~25 nm ), the contacting surfaces employ the shear energy introduced by the sliding motion to move grain boundaries and to reorient, rotate and elongate grains in order to create a coarsened third body layer with the <111> bcc packed direction aligned with the shearing direction. The enlarged reoriented interface grains are then capable of accommodating the sliding motion and deformation through dislocation and twin boundary nucleation and propagation. Shear bands and dynamic twin boundaries, oriented along the sliding direction and traveling perpendicular to the sliding motion within the coarsened grain region, enable the creation of shear planes which accommodate the sliding motion.

**[33] Unraveling and Eliminating Dissipation Mechanisms in Contacts of Polymer-Bearing Surfaces**

***S. de Beer**, E. Kutnyanszky, P. M. Schön, G. J. Vancso, M. H. Müser*

Polymer brushes are well known to lubricate high-pressure contacts, because they can sustain a high normal load while maintaining low friction at the interface. Depending on the contact-geometry, direction of motion and brush characteristics, different dissipation mechanisms dominate the friction forces. For example, in a parallel plate geometry the interdigitation of the opposing polymers determines the lubricity, while for spherical star polymers in relative motion, viscoelastic deformation governs the energy dissipation. We discuss the relative importance of the dissipation channels for real contacts and show via molecular dynamics simulations and atomic force microscopy measurements that, by using an asymmetric contact of two immiscible polymer brush systems, the important dissipation-mechanisms – interdigitation and capillary break-up – can be eliminated. Moreover, visco-

eleastic deformation is strongly reduced. For such immiscible polymer brush systems, we find that the friction upon sliding is a few orders of magnitude lower than for symmetric miscible contacts. Our developed system therefore holds great potential for application in industry.

**[34] redoxSQE – A Non-Equilibrium Charge-Transfer Method for Electrolytes and other Dielectric Materials**

***W. B. Dapp**, M. H. Müser*

In order to accurately calculate Coulomb forces in Molecular Dynamics (MD), it is vital to know the effective atomic charge on each atom. While there are several popular force fields (QE, AACT) for this task, they each have severe shortcomings. Split Charge Equilibration (SQE) is a method combining the beneficial aspects of both QE and AACT, while avoiding their deficiencies, such as predicting a wrong charge distribution among dissociation of dimers.
To date, partial atomic charges are either assumed constant or assigned according to minimization principles that are smooth and unique functions of the instantaneous atomic coordinates. Thus, charge-transfer history effects cannot be accounted for, as they occur for instance during contact-induced electron transfer between two solid bodies. In particular, redox reactions involve a quasi-discontinuous change of the electronic state, without significant atomic rearrangement.
We propose an extension to SQE, called redoxSQE, in which we assign discrete oxidation states to each atom. This enables us to model redox reactions, and to get a step closer to simulate all-atom batteries. In an initial proof-of-concept, many generic properties of macroscopic batteries are reproduced self-consistently. RedoxSQE can help to better understand the processes happening at the electrode-electrolyte interface.

**[35] *Ab Initio* Study of Structural and Electronic Properties of Rare-Earth Nickelates**

***K. Rushchanskii**, S. Blügel, M. Ležaic*

Ability of switching between metallic and insulating states by external factors is a very demanding property for industrial applications such as ferroelectric memories. In this sense, rare-earth nickelates are very promising materials due to their perovskite crystalline structure, which allows epitaxial growth of ultra-thin films on conventional ferroelectrics as oxide substrates. They exhibit metal-insulator (MI) transition, which could be continuously controlled by composition, bi-axial strain and (or) electric field. Theoretical description of this class of strongly correlated materials is quite challenging: *ab initio* results within DFT+U scheme fail to reproduce correct magnetic ground state, as well as the effect of epitaxial strain on MI transition temperature [1].
We present results of our comprehensive study of structural, magnetic and electronic properties of bulk $ReNiO_3$ (Re=Y, Gd, Eu, Sm, Nd and Pr) and strained $SmNiO_3$ films [2], performed within HSE06 functional [3]. We show correlation between MI transition temperature and structural parameters of bulk and films, which agrees well with the existing experimental data. We analyze the difference in the electronic structure obtained within DFT+U and hybrid functionals and the resulting ground state magnetic ordering. We discuss the obtained changes in the electronic structure of bulk materials and strained films and their correlation with experimental MI transition temperatures.
We acknowledge the support by Helmholtz Young Investigators Group Programme VH-NG-409, JSC and JARA-HPC.

References:
[1] S. Prosandeev, L. Bellaiche, J. Íñiguez, Phys. Rev. B 85, 214431 (2012).

[2] F.Y. Bruno, K.Z. Rushchanskii, S. Valencia, Y. Dumont, C. Carrétéro, E. Jacquet, R. Abrudan, S. Blügel, M. Ležaic, M. Bibes, and A. Barthélémy, Phys. Rev. B 88, 195108 (2013).
[3] J. Heyd, G.E. Scuseria, M. Ernzerhof, J. Chem. Phys. 124, 219906 (2006).

## [36] Multiscale Molecular Dynamics Study of Photoresponsive Azo-Materials

*J. Hekele, M. Boeckmann,* ***N. Doltsinis***

The photoswitchable polymer poly-disperse-orange-3-metacrylamide (PO3MAM) has been studied using a recently developed atomistic force field derived from nonadiabatic hybrid *ab initio*/classical force field (QM/MM) molecular dynamics. PO3MAM is a potential candidate for inscribing light-trapping patterns on the back surface of organic photovoltaic devices. Here we investigate the microscopic mechanism of such light-induced pattern formation by exposing a selected region of a PO3MAM surface to light while leaving the remaining region in the dark. It becomes clear that a large number photoisomerisation cycles per molecule are required to induce significant light-induced mass transportation that could result in surface structuring.

# Fluid Mechanics

### [37] Properties of Streamlines in Turbulent Channel Flows with Wavy Walls

***F. Hennig**, J. Boschung, N. Peters*

We investigate the turbulent velocity field by means of instantaneous streamlines. The streamlines are partitioned into segments and decompose the velocity field in a non-arbitrary way. The segments are defined by extreme points based on the velocity magnitude. The boundaries of all streamline segments define a surface in space where the gradient of the projected velocity in streamline direction $\partial u/\partial s$ vanishes. This surface contains all local extreme points of the velocity magnitude. Such points also include stagnation points of the flow field, which are absolute minimum points of the turbulent velocity field. The properties of the $\partial u/\partial s=0$ surface (and thus of stagnation points) are affected by local pressure gradients. Therefore, direct numerical simulations (DNS) of a turbulent flow with wavy walls, which induce complex pressure effects, are conducted. For the DNS a spectral element code is employed. The results have been validated against DNS and experimental data from literature. Based on the DNS the surface $\partial u/\partial s=0$ is investigated in detail and its interaction with streamlines is visualized.

### [38] Accelerating Turbulence Computations on JUQUEEN

***J. H. Göbbert**, M. Gauding, N. Peters*

Highly resolved direct numerical simulations of turbulence using Fourier pseudo-spectral methods is a computation and communication intensive application. As almost 100% of the communication and most of the computation time is consumed by the 3d Fast Fourier Transformations several techniques have been successfully combined for best performance and scaling. This includes overlapping of communication and computation based on non-blocking collective operations of MPI 3.0, multithreading and data reduction. Beside this we discuss the lessons learned in I/O and mapping and the most promising approach for the current production run.The new code enables the computation of an isotropic homogeneous forced turbulence on $6144^3$ grid points with a Taylor based Reynolds number of 700.

### [39] The Local Structure of Turbulent Flows at High Reynolds Numbers

***M. Gauding**, J. H. Göbbert, N. Peters*

Most understanding of turbulence at high Reynolds numbers is based on the scaling theory developed first by Kolmogorov (1941) and extended later to passive scalars by Obukhov (1949) and Corrsin (1951). Based on dimensional arguments, this theory relates the statistics of velocity or scalar increments to the mean energy or scalar dissipation. By the Kolmogorov-Obhukov-Corrsin (KOC) theory the information about the local structure of the turbulent field is lost when taking ensemble averages over fixed separation distances. This issue was overcome by Wang and Peters (2006,2008) by the theory of dissipation elements. Here, two-point statistics are calculated along gradient trajectories that connect local minimum and local maximum points in the scalar field. The spatial region formed by the ensemble of all gradient trajectories sharing the same extreme points is called dissipation element. They may be parameterized by the linear separation distance and the scalar difference between the extreme points. By this approach the linear separation distance itself becomes an intrinsic stochastic quantity that is determined by the turbulent field. Here, we propose to decompose the signal of a passive scalar along a straight line into piece-wise monotonously increasing or

decreasing line segments that start at a local minimum point and end at a local maximum point or vice versa. These line segments can be understood as one-dimensional dissipation elements. Thereby, we retain the property that the segmentation is determined intrinsically by the turbulent field and capture the local structure of the turbulent field. But because the segmentation is one-dimensional it can be easily related to conventional two-point statistics in the sense of the KOC theory.
We have conducted direct numerical simulations of turbulent scalar mixing with Taylor microscale based Reynolds number varying between 85 and 530. The computational method is based on a pseudo-spectral approach to solve the incompressibel Navier-Stokes equations as well as an advection-diffusion equation for a passive scalar. The biggest run has been conducted by using more than 68 billion collocation points. Based on this data base, statistics and scaling laws of line segments are computed and the results are compared to conventional two-points statistics. Additionally, line segments are used the establish a novel description of the physics behind cliff-ramp structures. We will show that the width of the steepest gradients is approximately 6 times the Kolmogorov length. Ramps in the scalar profile occur preferentially for descending segments which are oriented parallel to the mean scalar gradient. Finally, we will show how cliff-ramp structures are related to small-scale anisotropy.

**[40] Direct Numerical Simulation of Turbulent Flows with and without Chemical Reaction**

***M. Gauding**, J. H. Göbbert, F. Dietzsch, F. Hennig, C. Hasse, N. Peters*

Recent advances in high performance computing on massive-parallel systems enables us to conduct direct numerical simulations (DNS) of turbulent flows at high Reynolds numbers close to laboratory experiments. DNS has become an indispensable tool. It provides a complete description of the flow where the three-dimensional flow fields are known as a function of space and time. Generally, one aims at achieving the highest possible Reynolds number while resolving the smallest scales down to the Kolmogorov length.
We present the computational methods and principal results of three different types of direct numerical simulations, namely mixing of a passive scalar in homogeneous isotropic turbulence (case A), a turbulent evolving shear layer (case B), and a turbulent diffusion flame evolving in homogeneous isotropic turbulence (case C).
For case A the incompressible Navier-Stokes equations are solved in a periodic cubic box employing a highly efficient pseudo-spectral method. Parallelization is based on a hybrid MPI/OpenMP approach with a two-dimensional domain decomposition. The Taylor microscale based Reynolds number is varied between 88 and 529 where the biggest run uses more than 68 billion collocation points. These simulations resolve a wide range of different scales which enables us to analyze scaling laws and universal properties.
For case B results of a turbulent evolving shear layer solved on a grid with 4096x2048x1536 points are presented. The computational method is based on a sixth order implicit finite difference scheme and the pressure is solved exactly by means of a Helmholtz equation.
Case C employs similar computational methods as case B. However, in order to model non-premixed combustion an incompressible formulation is no longer valid. Transport equations of scalar fields now exhibiting a chemical source term which might locally lead to high heat releases. In addition, due to high values of the scalar dissipation rate and straining motions local extinction and reignition events must be considered. Therefore the Navier-Stokes equations are solved for Low-Mach number flows. Further, the DNS of reactive flows enables us to analyze small scale mixing properties as well as the impact of differential diffusion which in a laboratory framework are often difficult to access.

**[41] Highly-Resolved Numerical Simulations of Bed-Load Transport in a Turbulent Open Channel Flow**

*B. Vowinckel, T. Kempe,* ***J. Fröhlich***

The present study presents highly-resolved simulations of a turbulent open channel flow laden with up to 27000 spherical particles that are conveyed across a rough bed. The rough bed consists of fixed spherical particles of the same size arranged in hexagonal ordering. The mobility of the particles constituting the bed load is around its critical value, so that particles are constantly colliding either with each other or the fixed bed. The bulk Reynolds number of the flow is 2941, the flow depth is 9 particle diameters. The numerical method employs an Euler-Lagrange approach with an Immersed Boundary Method to resolve each individual particle with 22 grid points per diameter. Five different runs were carried out to investigate the role of mass loading and particle density, which are the key parameters of the problem. The computational domain is very large to allow particles to create bed form structures with high fidelity. The observed particle structures differ substantially between the runs by their scales in time and space. The results are in agreement with experimental evidence observed at higher Reynolds number.

**[42] Automated Optimization of Casing Treatments for Transonic Compressors**

***G. Goinis***

The working range of a gas turbine compressor is limited towards higher pressures by a phenomenon called surge. The occurrence of surge must be prevented under any circumstances as it can lead to massive flow instabilities and engine damage. An adequate surge margin (the range between working point and stability limit) has to be ensured at all times. This limitation often requires the compressor to run at sub-optimal efficiencies and can also have an impact on the design of a compressor, e.g. making it necessary to implement adjustable blade rows, bleed valves and even an increased number of stages. An effective extension of the surge margin can therefore result in compressors that operate more efficiently.
A notable surge margin enhancement can be achieved using so called casing treatments on transonic compressors. Casing treatments are geometric modifications of the casing above the rotor and mainly influence the flow in the tip region of the rotor, often the source for instabilities leading to surge. Casing treatments can have various shapes. One common type are axial slots which are subject to this study.
In order to analyze the correlations between efficiency, surge margin and other flow quantities on the one hand and the geometric parameters related to axial slots on the other, an automated multi objective geometry optimization of axial slots is performed. This involves the usage of time accurate CFD simulations for each new CT design the optimization tool proposes. In total many hundred different geometries are simulated. An automated optimization is therefore a task that requires a high level of computational resources.
The result of the optimization is a Pareto front with all optimal geometries regarding surge margin and efficiency. The working principles and flow phenomena of the Pareto-optimal axial slots are analyzed in detail to obtain a better understanding of the mechanisms leading to the extension in surge margin.

**[43] Numerical Studies of Small-Scale Turbulent Mixing**

***P. Götzfried****, B. Kumar, R. Shaw, J. Schumacher*

The turbulent entrainment and subsequent mixing of clear and cloudy air determines the

overall lifetime of clouds. We perform direct numerical simulations (DNS) to study these entrainment and mixing processes in detail. A hybrid numerical model is used which couples the Eulerian description of velocity, temperature and vapor mixing ratio with a Lagrangian model of a large cloud droplet ensemble. We find that the Damköhler number Da, a dimensionless parameter which describes the ratio of fluid time scale and a "reaction time scale", covers most essential aspects of the mixing process. Two limits of the entrainment can coexist on different spatial scales, the homogeneous (Da << 1) at small scales of turbulence and the inhomogeneous (Da >> 1) case at the largest scales. In the first case droplets change their radius by the same amount, in the other case a subset of droplets evaporate completely leaving other droplets unchanged. Another scope of our work is to investigate general statistics of moist air excluding liquid particles. Of general interest are the longitudinal velocity differences (velocity increments). At adjacent spatial points their probability density function (PDF) deviates from the Gaussian distribution as visible by exponential tails. This is a direct evidence of fine-scale intermittency. The tails broaden further if we increase the overall size of the simulation domain and therefore reach a higher Reynolds number.

**[44] High-Amplitude Fluctuations of Velocity and Temperature Gradients in Turbulent Convection**

***M. S. Emran**, J. Scheel and J. Schumacher*

We present high-resolution direct numerical simulation studies of turbulent Rayleigh-Benard convection in a closed cylindrical cell with an aspect ratio of one. Our emphasis is to unravel extreme fluctuations of the gradients of the turbulence fields in convection. One central question of turbulence research is if these fluctuations follow universal laws, independently of the large-scale driving mechanisms of turbulence. Therefore, our high-resolution studies are compared with simulation data from turbulent plane shear flows and homogeneous isotropic turbulence. We find indeed an agreement in the scaling laws for higher-order moments of the kinetic energy dissipation rate which are obtained in the bulk of the convection cell. The direct numerical simulations make use of a spectral element method which combines the flexibility of a finite element method with the spectral accuracy. We investigate the convergence properties of the spectral element method and verify that both dissipation fields are very sensitive to insufficient resolution. It also turns out that global transport properties and the energy balances are partly insensitive to such insufficient resolution and yield correct results even when the dissipation fields are underresolved. Our present numerical framework is also compared with high-resolution simulations which use a finite difference method. For most of the compared quantities the agreement is found to be satisfactory.

**[45] Direct Numerical Simulation of Turbulent Reacting Flows on Unstructured Grids and with Detailed Chemistry**

***F. Zhang**, H. Bonart, T. Zirwes, P. Habisreuther, H. Bockhorn*

The current work presents CFD (computational fluid dynamics) simulations of methane/air and hydrogen/air combustion by means of the direct numerical simulation (DNS) technique. This method solves the exact formulation of the balance equations for the total mass, the momentum in three spatial directions, the mass of each species, and the energy, employing detailed chemistry. It also resolves all time and length scales existing in turbulent flames. Therefore, a DNS is the most accurate but also the most CPU-intensive method. Until now DNS is only useful as a research tool, for example, to develop scaling laws and novel turbulence/combustion models for subordinate large eddy simulation (LES) or Reynolds Averaged Navier-Stokes (RANS) approaches.
The primary aim of the study is to justify the applicability of a new DNS solver for complex

three-dimensional problems by running it on high performance computing (HPC) facilities. The solver has been developed at the Engler-Bunte Institute/Division for Combustion Technology of the Karlsruhe Institute of Technology (KIT). It has been implemented into the open source code OpenFOAM and connects via a coupling library with the thermochemical libraries of Cantera. Thereby, OpenFOAM has the task to solve the conservation equations with the finite volume method, whereas the thermodynamic state in terms of pressure, temperature and species composition serves as the input parameter for the Cantera algorithms, which evaluate the necessary transport properties and the reaction rates needed for the solution of the governing equations in OpenFOAM.
The computational grids used for the DNS include up to 111 million finite volumes. The DNS cases have been run on the supercomputer JUQUEEN from JSC with up to 8192 cores. Therewith, a very good scaling behavior has been observed on the IBM Blue Gene/Q computing architecture. From this type of DNS it is possible to obtain a detailed characterization of turbulent combustion in three-dimensions, allowing deeper understanding of the interplay between turbulent fluctuations and flame propagations, which plays a significant role for the efficiency in modern combustion system.

**[46] Computer Simulation of Flow past Superhydrophobic Striped Surfaces**

***J. Zhou**, A. V. Belyaev, E. S. Asmolov, O. I. Vinogradova, F. Schmid*

We report results of Dissipative Particle Dynamics simulations for an anisotropic flow past superhydrophobic striped surfaces. We systematically vary several important parameters, such as the flow direction, the area fraction of the gas sectors, and the local slip length of the gas/liquid interface. We compare the simulation results with the numerical solution to the Navier-Stokes equations, analytic expressions, and asymptotic formulas in the limits where the local slip-length is small and large in comparison to the texture periodicity. The simulation results allow one to adjust surface properties to optimize transverse phenomena and passive microfluidic mixing. Our approach could be helpful to rational design of superhydrophobic surfaces.

**[47] High Performance Simulation of Wind Turbine Aeroelasticity**

***A. E. Öngüt**, M. Behr*

The research on renewable and sustainable energy gains momentum due to the facts such as the increasing energy demand, increasing energy prices and global warming. Wind energy is one of the promising renewable energy sources and wind energy industry grows rapidly in many countries. Current trend in wind energy industry is to make wind turbines larger and establish them in off-shore regions to increase the overall cost effectivity of energy production. As a result of this trend, loads acting on the wind turbine rotor and drive train also increase. This project, which is conducted together by the Chair for Computational Analysis of Technical Systems (CATS) and the Institute for Machine Elements and Machine Design (IME) of RWTH Aachen University, investigates active control methods to improve the wind turbine efficiency and alleviate the undesired loads acting on the turbine components.
In order to simulate the fluid structure interaction occurring due to the interaction of wind turbine rotor blades with the surrounding air, we follow a partitioned approach, which means that the flow and structural solvers are independent software tools and they are connected through a coupling module. This allows a more efficient development and validation procedure for both solvers. The CFD solver that is used during simulations is XNS, which is a highly parallel, stabilized FEM solver. The structural solver is “Finite Element Analysis for Aeroelasticity” (FEAFA) and both solvers are widely used and validated in previous studies. The coupling between two solvers is obtained with “Aeroelastic Coupling Module” (ACM),

which offers different coupling algorithms.
This poster focuses on the latest aeroelastic results obtained by CATS. First, a brief theoretical introduction to aeroelastic CFD simulations as well as the used software tools and their capabilities are given. Then, recent simulation results for rotor-only and complete-turbine configurations are illustrated both for aeroelastic and rigid cases. Results are compared with the available results in literature and a good agreement is observed [1,2]. The computation time used for the simulations is also evaluated, since the CFD solver requires high computing resources and all simulations are carried out on JUQUEEN supercomputing facility. At the end, conclusions are drawn and future plans are briefly discussed.

References:
[1] M.-C. Hsu and Y. Bazilevs. Fluid-structure interaction modeling of wind turbines: Simulating the full machine. to appear in Computational Mechanics, 2012.
[2] J. M. Jonkman, S. Butterfield, W. Musial, and G. Scott. Definition of a 5-MW reference wind turbine for offshore system development. National Renewable Energy Laboratory Colorado, 2009.

## [48] The Dynamics of Finite-Size Settling Particles

***T. Doychev**, M. Uhlmann*

We have investigated the gravity induced settling of finite-size particles in an ambient fluid by means of direct numerical simulation (DNS). Such configurations are relevant to a large number of applications such as meteorology, mechanical and environmental engineering. The problem is governed by three control parameters: (i) the particle-to-fluid density ratio $\rho_p/\rho_f$, (ii) the volume fraction $\Phi_s = V_p/V_l$ and (iii) the generalized Galileo number $Ga = \sqrt{|\rho_p/\rho_f - 1||\boldsymbol{g}|d_p^3}/\nu$, representing the ratio between the gravity and the viscous forces. The Galileo number and the particle-to-fluid density ratio characterize the regime of particles settling and in particular the particle wake (Jenny et al. 2004). A variety of motion patterns exist, from straight vertical to fully chaotic paths, for which the fluid motion in the near field around the particles and the particle wake play a dominant role (Ern et al. 2012). Therefore, the proper resolution of the flow field in vicinity of the particles is crucial. Here, the interface between the dispersed- and carrier-phase was fully resolved by means of an immersed boundary method (Uhlmann 2005). Particular care has been taken to meet the respective resolution requirements.
We have performed simulations of multiple particles settling in the steady oblique regime at the Galileo number $Ga = 178$. We have considered two different flow cases with different solid volume fractions. The problem is characterized by the parameter triplets $(\rho_p/\rho_f = 1.5, Ga = 178, \Phi_s = 0.005)$ and $(\rho_p/\rho_f = 1.5, Ga = 178, \Phi_s = 0.0005)$. Here the analysis will focus on two topics: (i) how mobility and the presence of multiple particles affect the wake properties of the particles and (ii) what is the spatial structure of the dispersed phase. We found out, that the particles exhibit strong inhomogeneous spatial distribution (i.e. they agglomerate into clusters) at both considered values of the solid volume fraction. It was observed that the particle clusters are preferentially oriented in the vertical direction. Additionally the particle-induced flow field is observed to be highly anisotropic with dominant vertical components and to experience characteristic features of pseudo-turbulent flows.

References:

P. Ern, F. Risso, D. Fabre, and J. Magnaudet. Wake-induced oscillatory paths of bodies freely rising or falling in fluids. Annu. Rev. Fluid Mech., 44:97–121, 2012.
doi: 10.1146/annurev-fluid-120710-101250

M. Jenny, J. Dušek, and G. Bouchet. Instabilities and transition of sphere falling or ascending freely in a newtonian fluid. J. Fluid Mech., 508:201–239, 2004.
doi: 10.1017/S0022112004009164

M. Uhlmann. An immersed boundary method with direct forcing for the simulation of particulate flows. J. Comp. Phys., 209:448–476, 2005.
doi: 10.1016/j.jcp.2005.03.017

**[49] Non-Linear Wave and Flow Dynamics of Laminar Three-Dimensional Falling Liquid Films**

*G. F. Dietze, **W. Rohlfs**, K. Nährich, R. Kneer, B. Scheid*

Full numerical simulations of the Navier-Stokes equations for four cases of vertically falling liquid films with three-dimensional surface waves have been performed. Flow conditions are based on several previous experimental studies where the streamwise and spanwise wavelengths were imposed, which we exploit by simulating periodic wave segments. The considered flows are laminar but approach conditions at which intermittent wave-induced turbulence has been observed experimentally (Re=75). Working liquids range from water to silicon oil and cover a large interval of the Kapitza number (Ka=18-3923), which relates tensile to viscous forces.
Simulations were performed on the supercomputer JUROPA, using a finite volume code and the volume of fluid and continuum surface force methods to account for the multiphase nature of the flow. Our results show that surface waves, consisting of large horseshoe-shaped wave humps concentrating most of the liquid and preceded by capillary ripples on a thin residual film, segregate the flow field into two regions: an inertia-dominated one in the large humps, where the local Reynolds number is up to five times larger than its mean value, and a visco-capillary region, where capillary and/or viscous forces dominate. In the inertial region, a complicated structure of small-scale vortices arises, which we believe to represent a path toward intermittent turbulence in falling liquid films. Conversely, the flow in the visco-capillary region of large Ka fluids is entirely governed by the local free surface curvature through the action of surface tension forces, which impose the pressure distribution in the liquid film. This results in flow separation zones underneath the capillary troughs and a spanwise cellular flow pattern in the region of capillary wave interference. In some cases, capillary waves bridge the large horseshoe humps in spanwise direction, coupling the two aforementioned regions and leading the flow to oscillate between three- and two-dimensional wave patterns. This persist over long times as has been confirmed by simulations with the low-dimensional model of Scheid et al. (J. Fluid Mech., vol. 562, 2006, p. 183), which we compare with our direct simulations. The governing mechanism is connected to the bridging capillary waves, which drain liquid from the horseshoe humps, decreasing their amplitude and
wave speed and causing them to retract in streamwise direction. Overall, it is observed that spanwise flow structures (not accounted for in two-dimensional investigations) are particularly complex due to the absence of gravity in this direction.

# Condensed Matter

### [50] Spatial and Temporal Propagation of Kondo Correlations

*B. Lechtenberg,* ***F. B. Anders***

We address the fundamental question how the spatial Kondo correlation build up in time assuming an initially decoupled impurity spi. We investigate the time-dependent spin-correlation function n the Kondo model with antiferromagnetic and ferromagnetic coupling after switching on the Kondo-coupling at time t=0. We present data obtained from a time-dependent numerical renormalisation group calculation. We gauge the accuracy of our two-band NRG by the spatial sum-rules of the equilibrium correlations functions and the reproduction of the analytically exactly known spin-correlation function of the decoupled Fermi-sea. We find remarkable buildup of Kondo-correlation outside of the light-cone defined by the Fermi-velocity of the host metal. By employing a perturbative approach exact in second-order of the Kondo coupling, we connect these surprising correlations to the intrinsic spin-density entanglement of the Fermi sea.

### [51] Singular Density of States and Frozen Multifractality in Graphene with Vacancy Disorder

*N. Weik, T. Mayer, V. Haefner, M. Walz, F. Evers*

Disorder plays a fundamental role in transport properties of graphene. We model a specific kind of disorder, vacancies, which introduce zero modes in the density of states (DOS) of graphene. The system has the peculiarity that the DOS is very sensitive at low energies to the detailed distribution of the vacancies. In this work, we study the DOS of graphene in a tight binding model with vacancies. Our focus is on compensated disorder, i.e. the case of an equal number of vacancies in both sublattices. In previous analytical studies, systems of chiral symmetry class BDI have been shown to exhibit a diverging DOS near the band center [1]. The goal of this work is to extend the numerical studies based on the lattice model to this regime in order to confirm these predictions. This energy regime is extremely interesting since it allows to study of phenomena such as frozen multifractality [1]. The optimized and parallelized wave-packet propagation method enabled simulations of the DOS for models with $10^8$ sites. For the DOS close to the band center we confirm divergent behavior predicted in an analytical study [2]. Multifractal analysis in the near-critical regime reveals freezing transitions of the wave functions.

References:
[1] F. Evers and A. D. Mirlin, Rev. Mod. Phys. 80, 1355 (2008).
[2] R. Gade, F. Wegner, Nucl. Phys. B 360, 213 (1991).

### [52] Correlated Electron States in Realistic Oxide Heterostructures

***F. Lechermann****, L. Boehnke, D. Grieger, C. Piefke*

The recent possibilities for designing materials beyond nature's original conception open a fascinating new chapter in condensed matter physics. Various interface architectures in oxide heterostructures are in this context intriguing sources of novel emerging physics. Ferromagnetism and/or superconductivity within originally band-insulating materials are prominent examples thereof.
In this poster an advanced theoretical effort to tackle these modern challenges on a realistic

level is presented. By means of the combination [1] of density functional theory (DFT) with explicit many-body methods, such as dynamical mean-field theory (DMFT), it becomes possible to address the intricate interplay between band-structure effects and electronic correlations on an equal footing, even for the named latest materials developments. Since this approach merges the sophisticated materials science aspect of large unit-cell structures with explicit quantum fluctuations, large numerical effort is needed. We will explicitly discuss the complex physics of $LaTiO_3/SrTiO_3$ superlattices [2] as well as new DFT+DMFT insight into the mechanism of itinerant ferromagnetism at the $LaAlO_3/SrTiO_3$ interface [3].

References:
[1] D. Grieger, C. Piefke, O. E. Peil and F. Lechermann, Phys. Rev. B 86, 155121 (2012).
[2] F. Lechermann, L. Boehnke and D. Grieger, Phys. Rev. B 87, 241101(R) (2013).
[3] F. Lechermann, L. Boehnke, D. Grieger and C. Piefke, arXiv:1401.6105 (2014) .

**[53] Energy Dissipation of Moved Magnetic Vortices**

***M. P. Magiera**, D. E. Wolf*

A two-dimensional easy-plane ferromagnetic substrate, interacting with a dipolar tip which is magnetised perpendicularly with respect to the easy plane is studied numerically by solving the Landau-Lifshitz Gilbert equation. The dipolar tip stabilises a vortex structure which is dragged through the system and dissipates energy [EPL 103, 57004 (2013)]. An analytical expression for the friction force in the $v \to 0$ limit based on the Thiele equation is presented. The limitations of this result which predicts a diverging friction force in the thermodynamic limit, are demonstrated by a study of the size dependence of the friction force. While for small system sizes the dissipation depends logarithmically on the system size, it saturates at a specific velocity-dependent value. This size can be regarded as an effective vortex size and it is shown how this effective vortex size agrees with the infinite extension of a vortex in the thermodynamic limit. A magnetic friction number is defined which represents a general criterion for the validity of the Thiele equation and quantifies the degree of nonlinearity in the response of a driven spin configuration.

**[54] Localization Length Critical Index in a Random Network Model for the Quantum Hall Effect**

***W. Nuding**, A. Klümper, A. Sedrakyan*

In the calculations of the critical index of a Chalker-Coddington network model of the plateau-plateau transitions in the Quantum Hall Effect the so far explored approaches show significant deviations from the experimental value. We introduce a Chalker-Coddington like class of models on random lattices with topological properties. With the resources of JUROPA we explore how the localization length index in the modified Chalker Coddington model changes.

**[55] Structures and Properties of Noble Metal Nanowires on Semiconductors: Si(111)-(5x2)-Au Surface**

***K. Seino**, F. Bechstedt*

Low-dimensional materials, their confined electron states lead to unusual conduction properties and phase transitions as a function of temperature, have become fascinating objects for solid-state physicists and material scientists. Besides their technological importance, they are expected to show interesting novel physics, including charge density

waves (CDW), spin density waves (SDW), as well as Mott-Hubbard metal-insulator transitions [1,2]. Moreover, in one-dimensional (1D) systems the physics can be drastically different from what is known from three-dimensional or two-dimensional matter. Even the Fermi liquid picture may be replaced by the Luttinger liquid one. It is fascinating to see how phase transitions between the conducting and insulating state are in fact driven by an electronic mechanism. In the case of a CDW, an electronic nesting condition governs the instability, while for a Mott-Hubbard transition the local Coulomb interaction comes into play.
Among the 1D metallic wire arrangements on flat and vicinal Si surfaces, the Si(111)-(5x2)-Au system is claimed to be understood. Several structural models were proposed for the Si(111)-(5x2)-Au surface by several techniques [3,4]. However, no consensus has yet been achieved on the atomic structure model. The recently revised experimental determination of the gold coverage as 0.6 monolayer (ML) obviously calls for a revised structural model as well [5]. However, based on results of diffraction experiments a new model was proposed recently [6].
We report results of *ab initio* calculations for the Si(111) surface with a 0.6 ML Au decoration including spin polarization effects. Different variations of the recently developed basic models are studied in detail. We also used different exchange correlation functionals including the Perdew-Becke-Ernzerhof functional for solids and surfaces (PBEsol) and the van der Waals density functional (vdW-DF). We clearly favor the model proposed by Erwin et al. [5] versus that proposed by Abukawa and Nishigaya [6]. Adatoms give a further stabilization. Spin polarization does not further lower the total energy. The resulting electronic structure agrees with the available experimental data.

References:
[1] P. C. Snijders and H.H. Weitering, Rev. Mod. Phys. 82, 307 (2010).
[2] S. Hasegawa, J. Phys. Condens. Matter 12, R463 (2000).
[3] J.D. O'Mahony, C.H. Patterson, J.F. McGilp, F.M. Leibsle, P. Weightman and C.F.J. Flipse, Surf. Sci. 277, L57 (1992).
[4] H. S. Yoon, J. E. Lee, S. J. Park, I.-W. Lyo and M.-H. Kang, Phys. Rev. B 72, 155443 (2005).
[5] S.C. Erwin, I. Barke and F. J. Himpsel, Phys. Rev. B 80, 155409 (2009).
[6] T. Abukawa and Y. Nishigaya, Phys. Rev. Lett. 110, 036102 (2013).

**[56] Multicanonical Analysis of the Gonihedric Ising Model: Non-Standard Scaling Behavior of First-Order Phase Transition**

*M. Mueller, **W. Janke**, D. A. Johnston*

The gonihedric Ising model originates from catching basic properties of fluctuating random surfaces in a bosonic string theory. Formulated as a lattice model of interacting classical spins it has been investigated by means of multicanonical Monte Carlo computer simulations to resolve open questions on its first-order phase transition. We note that the standard inverse system volume scaling for finite-size corrections at a first-order phase transition (i.e., $1/L^3$ for an $L\times L\times L$ lattice in $3\mathrm{D}$ ) is transmuted to $1/L^2$ scaling if there is an exponential low-temperature phase degeneracy. Our high-precision data provides strong confirmation of the predicted non-standard finite-size scaling law. The transition temperature has been determined consistently for the original plaquette model and its dual representation. Also the interface tension has been obtained for both models for the first time.

References:
M. Mueller, W. Janke, and D. A. Johnston, Non-Canonical Finite-Size Scaling at First-Order Phase Transitions, preprint arXiv:1312.5984 (cond-mat.stat-mech).

**[57] Electron Traps at the Ice Surface**

***M. Bockstedte**, A. Michl*

Water, water clusters and ice possess the fascinating ability to solvate electrons. On the surface of water cluster[1] and thin crystalline ice layer deposited on a metal substrate [2] long-living solvated electron states were observed that evolve from pre-existing surface traps. The identification of initial electron traps provides important insight into the electronic structure of the water surface, ice layers on metals and the dissociative interaction of electrons with adsorbates. Theoretical models [2] based on the bilayer terminated Ih-(0001) surface related such traps to orientational defects or vacancies with dangling OH-groups [3]. So far, a conclusive microscopic model of the electron traps at the surface of water structures on metals is missing. Here we address such electron traps including also water ad-structures observed by STM [4] theoretically using hybrid density functional theory and many-body perturbation theory in the G0W0 approximation. We identify a hierarchy of traps with increasing vertical electron affinity, ranging from water admolecules and hexagon adrows via clusters of orientational defects to vacancy-related traps.

References:
[1] Siefermann and Abel, Angew. Chem. Int. Ed. 50, 5264 (2011).
[2] Bovensiepen et al., J. Chem. Phys. C 113, 979 (2009).
[3] Hermann et al., J. Phys. cond. matter 20, 225003 (2008).
[4] Mehlhorn and Morgenstern, Phys. Rev. Lett. 99, 246101 (2007).

**[58] Light Propagation in Silicon-Based Thin-Film Solar Cells Investigated by Near-Field Microscopy and Rigorous Optical Simulation**

***M. Ermes**, A. Hoffmann, S. Lehnen, R. Carius, K. Bittkau*

Silicon-based thin-film solar cells yield reasonable efficiencies using abundant, non-toxic materials. Due to economic reasons and to save resources, however, the thicknesses of the active layers are much thinner than the absorption length of the incident light. Therefore, textured front contacts are used to scatter the incident light into large angles, thus coupling into guided modes, resulting in a prolonged optical path length.
To understand the light propagation inside the cell, we combine experimental and simulation methods to investigate these guided modes inside the layers of a solar cell.
Experimentally, scanning near-field optical microscopy (SNOM) is used. Here, a metal coated fibre tip with a small aperture scans across the textured surface of a sample while it is illuminated from the other side, therefore enabling us to investigate near-field effects above the sample. These near-field effects indicate the presence of guided modes, which are beneficial to cell performance. However, light propagation inside the sample is not directly accessible via experiment. Therefore, we use the Finite-Difference Time-Domain (FDTD) method to solve Maxwell's equations to calculate the light intensity distribution inside the structure at a nano scale to reproduce and support the experiment. Since the measured areas in the experiment can be as large as 10x10 µm², we need to simulate the same sample size, and therefore need high-performance computing resources.
However, when comparing the light intensity distribution obtained by experiment to that obtained by simulation at a constant distance of 20 nm above the surface, we see significant differences, especially far less near-field effects in the experiment. One explanation is the finite size of the tip, which does not allow for a constant surface to aperture distance of 20 nm. This is an effect also known as topography artefact.
To include this effect in simulations, one simulation is necessary for each measurement point. With each measurement consisting of 90000 points, however, this would lead to extreme amounts of computation time used for a single comparison.

We present a post-processing algorithm for application on a simulation without the tip that applies any topography artefacts caused by an idealised tip geometry to significantly enhance agreement between simulation and experiment. The better agreement indicates that topography artefacts are the main cause of difference between simulation and experiment for the structures we investigated.
Additionally, simulations were performed using idealised structures, both with (disturbed= and without (undisturbed) the tip included in the simulation domain. The results from comparing the light intensity of the undisturbed system to that inside the tip of the disturbed system further supports our post-processing algorithm.
The presented approaches are applicable for any kind of SNOM measurement and are not restricted to the investigation of thin-film solar cells.

**[59] Towards Steady-State Transport through a Quantum Dot at Finite Bias**

***T. Treffon**, E. Canovi, A. Moreno, A. Muramatsu*

We consider the steady-state transport through an interacting resonant level model. Based on the principle of maximum entropy we construct a time-independent density matrix that in the non-interacting limit reduces to the one advanced by Hershfield [1]. Naturally, we calculate transport through an impurity between two reservoirs in the grand canonical ensemble. To do so, we have to introduce ancilla states, such that a statistical mixture can be obtained from a pure state [2]. Using t-DMRG [3,4] with this enlarged Hilbert space we start at temperature T=8 in the maximal entangled state of the physical sites and the ancilla sites. Evolving this state in imaginary time allows us to obtain the steady-state at a given finite temperature.

References:
[1] S. Hershfield, Phys. Rev. Lett. 70, 2134 (1993).
[2] A. E. Feiguin and S. R. White, Phys. Rev. B 72, 220401 (2005).
[3] A. J. Daley, C. Kollath, U. Schollwöck, and G. Vidal, Journal of Statistical Mechanics: Theory and Experiment 2004, P04005 (2004).
[4] S. R. White and A. E. Feiguin, Phys. Rev. Lett. 93, 076401 (2004).

# Elementary Particle Physics

### [60] Maximally Twisted Mass Lattice QCD Calculations at the Physical Point

*A. Abdel-Rehim, C. Alexandrou, Ph. Boucaud, F. Burger, N. Carrasco, M. Constantinou, A. Deuzeman, P. Dimopoulos, V. Drach, X. Feng, R. Frezzotti, G. Herdoiza, G. Hotzel, K. Jansen, C. Kallidonis,* ***B. Kostrzewa****, G. Koutsou, M. Mangin-Brinet, I. Montvay, D. Palao, M. Petschlies, G.C. Rossi, F. Sanfilippo, L. Scorzato, A. Shindler, C. Urbach, U. Wenger*

Up until recently, lattice QCD calculations were carried out using a number of unphysically large pion masses with a subsequent extrapolation of measurements to the physical pion mass point. For certain observables, this extrapolation can be the dominant source of systematic error. Algorithmic advances and the availability of Petascale supercomputers have made it possible to simulate directly at the physical pion mass point, eliminating this source of systematic error.
In this contribution, a selection of preliminary results at the physical point from simulations by the European Twisted Mass Collaboration are presented. An overview of the lattice QCD action that was used is given and new features of the tmLQCD simulation software are presented together with some benchmark results. In addition to masses and decay constants of mesons involving light, strange and charm quarks, preliminary measurements in the nucleon sector are shown. Finally, a computation of the hadronic contribution to the anomalous magnetic moment of the muon is presented.

### [61] SU(3) Flavor Symmetry Breaking and Open Charm States

*R. Horsley, Y. Nakamura, D. Pleiter, P. E. L. Rakow,* ***G. Schierholz****, J. Zanotti*

By extending the SU(3) flavor symmetry breaking expansion from up, down and strange sea quark masses to partially quenched valence quark masses we propose a method to determine charmed quark hadron masses. Initial results for some open charmed pseudoscalar meson states and singly and doubly charmed baryon states are encouraging and demonstrate the potential of this procedure.

### [62] More Results on Finite Temperature QCD with Wilson Fermions

*S. Borsányi, S. Dürr, Z. Fodor, C. Hoelbling, S. D. Katz, S. Krieg, D. Nógrádi, K. K. Szabó,* ***B. C. Tóth****, N. Trombitás*

We investigate 2+1 flavor QCD thermodynamics using dynamical Wilson fermions in the fixed scale approach. Our previous study at a pion mass of 545 MeV is extended with two additional pion masses, approximately 440 MeV and 280 MeV. We perform simulations using 3 or 4 lattice spacings at each fixed pion mass and measure the renormalized chiral condensate, strange quark number susceptibility and Polyakov loop as a function of the temperature. We observe a decrease in the light chiral pseudo-critical temperature as the pion mass is lowered while the pseudo-critical temperature associated with the strange quark number susceptibility or the Polyakov loop is only mildly sensitive to the pion mass. These findings are in agreement with previous results obtained in the staggered formulation.

# Astrophysics

### [63] Survey of Type Ia Supernova Explosion Models

***S. T. Ohlmann**, M. Kromer, M. Fink, R. Pakmor, I. R. Seitenzahl, S. A. Sim, F. K. Röpke*

Type Ia supernovae are supposed to be thermonuclear explosions of white dwarfs consisting of carbon and oxygen. The remarkable uniform behaviour of their light curves allows their usage as standardizeable candles for distance measurements in cosmology. This standardization is reached using the Phillips relation - a relation between the width of the light curve and the total luminosity. The question of the detailed nature of the progenitor systems is still not settled - despite tremendous efforts in observation and modeling; also due to the fact that no progenitor system has been observed so far. In the delayed detonation model of Chandrasekhar mass white dwarfs, an initial subsonic deflagration turns into a supersonic detonation. One key parameter in this thermonuclear explosion is the initial composition governing the amount of energy being released, thus influencing the velocity distribution of the ejecta. This results mainly in a different evolution of the light curve and in different line velocities in the spectra.
In our group, a modeling pipeline has been established consisting of hydrodynamic simulations of the explosion phase, detailed nucleosynthesis calculations and subsequent radiative transfer computations. This links modeling to observations and allows to compare explosions in different progenitor models to observations.
In this project, this pipeline has been used to examine the impact of the initial composition of the progenitor white dwarf: the hydrodynamics of the burning fronts are altered in a way that for lower carbon mass fractions, they develop weaker with a lower energy release. This leads to an overall reduction in the amount of Ni56 produced in the explosion for lower carbon mass fractions. For the same amount of Ni56, the ejecta possess less kinetic energy, but the differences in velocity distributions and line velocities in spectra are small. Comparing a series of models with different initial carbon mass fractions, a range of Ni56 masses and thus maximum luminosities is produced. Since the light curve width does not follow the Philipps relation, the initial composition is supposed to be a secondary parameter driving the light curve-width relation orthogonal to the Philipps relation.

### [64] SN 2010lp - a Type Ia Supernova from a Violent Merger of Two Carbon-Oxygen White Dwarfs

***W. Hillebrand***

SN 2010lp is a subluminous Type Ia supernova (SN Ia) with a slowly-evolving lightcurve. Moreover, it is the only subluminous SN Ia observed so far that shows narrow emission lines of OI in late-time spectra, indicating unburned oxygen close to the centre of the ejecta. Most explosion models for SNe Ia cannot explain the narrow OI emission. Here, we present hydrodynamic explosion and radiative transfer calculations showing that the violent merger of two carbon-oxygen white dwarfs of 0.9 and 0.76 solar masses, respectively, adequately reproduces the early-time observables of SN 2010lp. Moreover, our model predicts oxygen close to the centre of the explosion ejecta, a pre-requisite for narrow OI emission in nebular spectra as observed in this supernova.

**[65] Environmental Effects on Planet Formation in the Cluster Expansion Phase**

*M. Steinhausen,* ***S. Pfalzner***

Most stars do not form in isolation but as part of a group of stars. Investigations of the effect of stellar encounters on protoplanetary discs have demonstrated its importance in dense environments during the early embedded cluster evolution. However, star cluster infant mortality suggests that a large fraction of the massive clusters dissolves within a few Myr, while only a small fraction survives the expulsion of the residual gas. In this study N-body simulations have been performed to investigate various expulsion scenarios. Hereby, the focus is on the significance of stellar encounters (i) before the remnant gas is expelled, (ii) during the expansion phase, and (iii) after the re-virialisation. It is shown that during the embedded phase multiple eccentric encounter events are dominating, preferentially in the dense inner cluster regions. The gas expulsion at the end of the star formation process leads to a rapid expansion of the cluster and a significant reduction of the fraction of bound stars. It is shown that in general unperturbed stars, located in the outer cluster regions, are expelled from the cluster, while a large fraction of highly disturbed stars in the central cluster parts remain bound. Consequently, encounters during the crucial first Myr of cluster development significantly shape the disc properties of the remnant cluster. Moreover, stars that are dispersed in the field are more suitable for planet formation, since they maintain their discs for a substantially prolonged timespan.

**[66] Planetesimal Formation in Protoplanetary Disks**

***K. Dittrich****, H. Klahr, A. Johansen*

Recent numerical simulations show long lived sub- and super-Keplerian flows in protoplanetary disks. These so-called zonal flows are found in local as well as global simulations of magneto-rotationally unstable disks. The resulting gas over- and under-densities have a radial size of 5 local pressure scale heights, and are stable for several tens of orbits. This is the first study about the effects of zonal flows on dust particles. Centimeter sized particles reach a hundred-fold density enhancement without self-gravity. The newest simulations show that the initial asteroid size distribution can be understood with dust clouds of realistic particle concentrations in zonal flow simulations.

**[67] Plasma and Dust Simulations of the Geysers of Saturn's Moon Enceladus**

***P. Meier****, H. Kriegel, U. Motschmann, J. Schmidt, F. Spahn*

A wide range of methods is available to numerically model space plasma processes. Dealing with scales comparable to ion gyration radii (e.g. comets, Titan or Enceladus), a hybrid model is the most convenient choice. It treats the electrons as a fluid, whereas a completely kinetic approach is retained to cover ion dynamics. From the numerical point of view, it can be categorized as a particle-mesh code. The particles which represent the ions interact with the electromagnetic fields defined on the numerical mesh.
Enceladus is a moon within Saturn's E-ring embedded in a plasma environment. Measurements of Cassini spacecraft have shown that water vapor and icy dust particles are ejected from the south polar regions through geysers. They form a plume towering Enceladus' south pole and escaping grains supply the E-ring. Cassini's Cosmic Dust Analyzer (CDA) can detect dust until a lower threshold of micrometers of radii. Data of Cassini Plasma Spectrometer (CAPS) show dust of nanometer size. On the one hand, the nanograins are affected by the plasma environment. On the other hand, the plasma is crucially modified by the feedback of the grains. Therefore, we iteratively perform plasma and dust simulations

achieving a consistent configuration. The results are compared with multiple Cassini data and a global picture of Enceladus' plume and its mutual interaction is developed. The perturbation of the electron and ion densities due to dust is studied. Finally, the dust grain distribution is reconstructed from the plasma measurements even beyond the regions covered by the Cosmic Dust Analyzer.

**[68] The Plasma Environment of the Comet 67P/Churyumov-Gerasimenko**

***C. Götz**, C. Koenders, K.-H. Glaßmeier*

In 2014, the European spacecraft Rosetta will arrive at the comet 67P/Churyumov-Gerasimenko, where it will deliver the PHILAE lander and start to escort the comet to its perihelion. The instrument package onboard gives a deeper insight into the evolution of the complex interaction between a comet and the solar wind. Previous simulations have focused on determining positions of boundaries in the cometary plasma environment under constant solar wind conditions to aid in the planning of Rosetta's trajectory around the comet.
However, while the comet is approaching the sun it will frequently cross the Heliospheric Current Sheet and experience dynamic solar wind conditions such as sudden magnetic field reversals. Simulations including these conditions will allow us to study the impact on the cometary plasma environment and therefore provide a look forward to the Rosetta measurements.

# Computational Plasma Physics

### [69] Interplay between Ionization, Pulse Propagation and Particle Acceleration in Intense Laser-Matter Interaction

***T. Liseykina**, M. Tamburini, D. Bauer*

Using three-dimensional, relativistic particle-in-cell simulations with ionization included we study the interplay between ionization, pulse propagation and particle acceleration in intense laser-matter interaction.
Of particular interest is the laser intensity and frequency regime for which initially transparent, wavelength-sized targets are not homogeneously ionized and the charge distribution changes both in space and in time on a sub-cycle scale. We found that a strong near-infrared or optical laser pulse interacting with an initially neutral, wavelength-sized helium-droplet may generate a charge density distribution that neither is homogeneous throughout the droplet nor concentrated only within a thin skin layer at the surface. Instead, oscillating electric fields may penetrate into the droplet interior under a certain angle, ionize, and propagate further in the just generated plasma [1]. This effect is attributed to the local field enhancements at the droplet surface predicted by standard Mie theory [2]. Furthermore we studied the interaction of moderately intense laser pulse with small initially homogeneous and neutral hydrogen-droplets for the range of parameters relevant to the corresponding parameters in the recent FLASH TS experiments. We found that the field enhancement at the droplet surface gets clearly imprinted in the structure of the surface ion density at the time scale of ~100 fs. Our preliminary results indicate that it might be possible to identify this structure by scattering experiments in IR-pump/short-wavelength FEL-probe setups at FLASH.
A wide range of novel studies in nonlinear optics as well as the major new regimes of extreme field physics require laser pulses which simultaneously exhibit three key features: few-cycle duration, high-energy and ultrahigh intensity. We studied a new scheme for the generation and control of a very intense, very short laser pulse with a “flying mirror” which reflects and focuses an intense laser pulse [3]. The resulting reflected pulse is shorter and more intense than the source pulse. We found that in order to maximize the peak intensity and the energy of the reflected pulse it is convenient to employ a heavy and therefore relatively slow “mirror”. This counter-intuitive result is explained by the larger reflectivity of a heavier “mirror”, which compensates for its lower velocity. Our simulations indicated the feasibility of the presented set-up by employing next-generation multi-PW laser systems.

References:
[1] T. Liseykina and D. Bauer, Phys. Rev. Lett 110, 145003 (2013).
[2] Max Born and Emil Wolf, Principles of Optics (Cambridge University Press, 2003).
[3] M. Tamburini, A. Di Piazza, T.V. Liseykina and C.H. Keitel// to be published in Phys. Rev. Lett. [arXiv:1208.0794].

### [70] Controlled Electron-Beam Injection into Plasma Waves for Tailored Betatron-Radiation Generation

***T. Mehrling**, R. A. Fonseca, J. Grebenyuk, J. L. Martins, A. Martinez de la Ossa, J. Vieira, L. O. Silva, J. Osterhoff*

Plasma-based accelerators offer gradients of far more than 10 GV/m but have not reached beam qualities and stabilities as required for common applications yet. Crucial for the quality and stability of the produced beams is their injection process into the plasma wave. In addition, a high degree of control over this process offers the possibility of steering the injection mechanism in a way which induces coherent betatron oscillations of the beam in the

plasma wave. Similar as in undulators, the electrons then emit radiation in the X-ray wavelength which is tunable by the injection process and suitable for applications such as phase-contrast imaging of biological specimens.
We present results of simulations, performed with the massively parallel 3D Particle-In-Cell (PIC) code OSIRIS on JUQUEEN. Two novel injection mechanisms are introduced. One technique directly uses the plasma-wakefield for ionization of a dopand gas and trapping of the released electrons and another method utilizes external static magnetic fields to relax trapping thresholds. These techniques have the potential of producing beams with high quality and stability in beam-driven plasma acceleration. Simulation results of induced betatron X-ray emission, steerable by external magnetic fields are demonstrated. Moreover, we present simulations of beam-injection by means of plasma-density transitions, featuring beams with ~100 nm scale emittance and studies on the evolution of the beam-emittance in staged plasma acceleration.

**[71] Thomson Scattering on Laser-Driven Targets**

***P. Sperling****, T. Bornath, T. Döppner, S. H. Glenzer, M. Harmand, S. Toleikis, T. Tschentscher, U. Zastrau, R. Redmer*

Free electron lasers enable new pump-probe experiments to characterize warm dense matter, i.e. systems at solid-like densities and temperatures of several eV. Such extreme conditions are relevant for the interior of giant planets and along the compression path of inertial confinement fusion capsules and can be investigated within pump-probe experiments. For instance, a short-pulse optical laser irradiates a carbon foil target that is subsequently probed with brilliant x-ray radiation. The inhomogeneous plasma prepared by the optical laser is specified with particle-in-cell simulations and the influence of impact ionization processes is investigated.
For the pump-probe experiments on carbon foils, we calculate the respective scattering spectrum based on the Born-Mermin approximation for the dynamic structure factor considering the full density and temperature dependent Thomson scattering cross section throughout the inhomogeneous target. We can identify plasmon modes characterizing the generated plasma and monitor their temporal evolution. The methods described here can be applied to various pump-probe scenarios by combining optical lasers, soft and hard x-ray sources, and are suited for campaigns planned at the MEC end station at LCLS in order to determine the plasma parameters of matter under extreme conditions.

# Computer Science and Numerical Mathematics

### [72] Scalability Analysis and Efficient Implementation of Numerical Algorithms

***M. Korch**, T. Rauber*

Most of today's computing systems are parallel in nature. The number of processor cores per system increases steadily. High-end supercomputers contain tens or hundreds of thousands of processing elements, and even smartphones are equipped with quad-core CPUs. This development generates an urgent demand for software that can exploit this potential for parallelism, and it is important to be able to use today's supercomputer systems to do research on parallelism, so that the software required for tomorrow's mainstream computer systems can be developed and be made available to the users in time.
Our working group searches for new algorithms, data structures and implementation techniques that can make efficient use of the resources provided by modern parallel computer systems. Focus is put on numerical algorithms, because often they are particularly computationally demanding on their own or they are part of other computationally intensive algorithms.
A major part of the computing time granted on JUROPA has been used to investigate efficient algorithms and software for the parallel solution of initial value problems (IVPs) of systems of ordinary differential equations (ODEs). The numerical solution of such problems can be highly computationally intensive, in particular if the dimension of the ODE system is large. Our project aims at a systematic scalability analysis of algorithms for the parallel solution of ODE IVPs. The results of these analyses are then used to improve the preexisting algorithms investigated and to develop new algorithms which can be executed efficiently on modern parallel computer systems by exploiting different types of parallelism (task, data, mixed parallelism) and by improving the locality of memory references and the communication patterns.
A second target of our computing time project is the development of scalable Particle-in-Cell (PIC) codes for astrophysical simulations of the time evolution of galaxies and globular clusters and the formation of black holes and spacetime singularities, based on the Vlasov-Poisson and Einstein-Vlasov systems, respectively, which is a cooperation with the mathematical physics group of the University of Bayreuth (Gerhard Rein). We have started with a step-by-step shared-memory parallelization of the Vlasov-Poisson code using POSIX Threads and later developed message passing codes using MPI. The MPI codes have been investigated on JUROPA using up to 4096 cores, and (weak) speedups up to 1280 have already been reached. The speedup obtained through parallelization has already helped in finding new numerical results, such as oscillating solutions of the Vlasov-Poisson system.

### [73] Towards the Automatic Generation of Efficient Geometric Multigrid Solvers for Exascale Computing

***S. Kuckuk**, S. Kronawitter, A. Grebhahn, C. Schmitt, H. Rittich, H. Köstler*

Multigrid methods provide solutions with optimal computational complexity for many PDEs. However, to achieve optimal complexity, the concrete algorithm needs to be adapted to the problem at hand. Furthermore, obtaining an efficient implementation requires the application of optimizations specific to the target hardware, a task that puts a significant burden on domain experts.
Project ExaStencils addresses this challenge by developing a code generation framework for specialized and highly tuned geometric multigrid solvers. It employs an intuitively usable DSL (domain-specific language) interface, automatically tuned communication patterns and stencil applications, as well as a way of optimizing relevant parameters via an SPL (software product

line) approach.
A first step towards this ambitious goal is the implementation of prototype stencil codes. The first application solves a 2D finite difference discretization of a representable elliptic PDE, in our case Poisson's equation, using HHG (hierarchical hybrid grid) data structures. A second code solves a 3D version of the same problem on a regular grid. The third program is mainly used to examine advanced hardware-dependent performance optimizations as, e.g., 3.5D blocking. With these three codes, we can already collect valuable data used for learning performance characteristics, checking convergence rate predictions and setting up feature models. The feature model approach allows for an efficient prediction, and thus optimization, of the execution time on the basis of only a few selected experiments.

**[74] Hierarchical Hybrid Multigrid Solver for the Stokes System**

***H. Stengel****, M. Huber, B. Gmeiner, U. Rüde*

In this presentation, we use the abstract concept of hierarchical hybrid grids to design scalable and fast multigrid solvers for the incompressible Stokes system that leads to a saddle point formulation. Complex applications may require extremely fine resolution easily resulting in systems of equations with more than a trillion unknowns. Even on the most advanced supercomputers this is a highly non-trivial and challenging task, since asymptotically optimal solvers are not automatically fast. The flexible and general hierarchical hybrid grids software framework and a quantitative performance analysis are the basis of excellent node performance and good scalability to almost a million parallel threads. We introduced an innovative performance model for the computational kernels in combination with the communication overhead. Weak and strong scaling properties are presented and show the applicability of our solver in case of extreme resolutions.

# Participants

| Name | First Name | Affiliation | City | Poster No. |
|---|---|---|---|---|
| Anders | Frithjof | Technische Universität Dortmund | Dortmund | 50 |
| Ansorge | Cedrick | Max-Planck-Institute for Meteorology | Hamburg | |
| Baumann | Tobias | Johannes Gutenberg Universität Mainz | Mainz | |
| Beck | Andrea | Universität Stuttgart | Stuttgart | |
| Beck | Teresa | IWR, Uni Heidelberg | Heidelberg | 1 |
| Beridze | George | Forschungszentrum Jülich | Jülich | |
| Biermann | Peter | Max Planck Gesellschaft | Bonn | |
| Binder | Kurt | Johannes Gutenberg Universität Mainz | Mainz | |
| Bleicher | Marcus | Goethe-University | Frankfurt/Main | |
| Bockstedte | Michel | Universität Erlangen-Nürnberg | Erlangen | 57 |
| Boeck | Thomas | TU Ilmenau | Ilmenau | |
| Böckmann | Marcus | Uni Münster | Münster | |
| Bolten | Matthias | Bergische Universität Wuppertal | Wuppertal | |
| Borsanyi | Szabolcs | Bergische Universität Wuppertal | Wuppertal | |
| Boschung | Jonas | RWTH Aachen University | Aachen | |
| Brehm | Martin | University of Leipzig | Leipzig | 28 |
| Breslau | Andreas | Max-Planck-Institut für Radioastronomie | Bonn | |
| Cong | Xiaojing | GRS and Forschungszentrum Jülich | Jülich | 22 |
| Coto | Pedro B. | Friedrich-Alexander Universität | Erlangen | 25 |
| Dabrowski | Jarek | IHP | Frankfurt/Oder | |
| Dapp | Wolf | Forschungszentrum Jülich | Jülich | 34 |
| de Beer | Sissi | University of Twente | Enschede | 33 |
| De Raedt | Hans | University of Groningen | Groningen | |
| Dibenedetto | Domenica | GRS | Aachen | |
| Dietzsch | Felix | TU Bergakademie Freiberg | Freiberg | |
| Dittrich | Karsten | Max Planck Institute for Astronomy | Heidelberg | 66 |
| Doltsinis | Nikos | Uni Münster | Münster | 36 |
| Doychev | Todor | Karlsruhe Institut für Technologie | Karlsruhe | 48 |
| Drzycimski | Kevin | Forschungszentrum Jülich | Jülich | |
| Emran | Mohammad | Ilmenau University of Technology | Ilmenau | 44 |
| Ermes | Markus | Forschungszentrum Jülich | Jülich | 58 |
| Fröhlich | Jochen | TU Dresden | Dresden | 41 |
| Gauding | Michael | RWTH Aachen University | Aachen | 39, 40 |
| Goergen | Klaus | Forschungszentrum Jülich | Jülich | 8 |
| Göbbert | Jens Henrik | RWTH Aachen University | Aachen | 38 |
| Götz | Charlotte | Technische Universität Braunschweig | Braunschweig | 68 |
| Götzfried | Paul | Ilmenau University of Technology | Ilmenau | 43 |
| Gohlke | Holger | Heinrich-Heine-University | Düsseldorf | 16 |
| Goinis | Georgios | German Aerospace Center (DLR) | Köln | 42 |
| Gottlöber | Stefan | Leibniz-Institut für Astrophysik Potsdam | Potsdam | |
| Gregroy | Eric | Bergische Universität Wuppertal | Wuppertal | |

| Name | First Name | Affiliation | City | Poster No. |
|---|---|---|---|---|
| Grotendorst | Johannes | Forschungszentrum Jülich | Jülich | |
| Gruner | Markus | University of Duisburg-Essen | Duisburg | 30 |
| Hanke | Christian | Heinrich-Heine-University Düsseldorf | Düsseldorf | 17 |
| Hennig | Fabian | RWTH Aachen University | Aachen | 37 |
| Höfler-Thierfeldt | Sabine | Forschungszentrum Jülich | Jülich | |
| Hohenadler | Martin | University of Würzburg | Würzburg | |
| Hossfeld | Friedel | Forschungszentrum Jülich | Jülich | |
| Hsu | Hsiao-Ping | Johannes Gutenberg-Universität Mainz | Mainz | 12 |
| Jahn | Sandro | Deutsches GeoForschungsZentrum | Potsdam | 4 |
| Jalkanen | Jari | Forschungszentrum Jülich | Jülich | |
| Janke | Wolfhard | Universität Leipzig | Leipzig | 56 |
| Jitsev | Evgueni | Forschungszentrum Jülich | Jülich | |
| Jones | Robert | Forschungszentrum Jülich | Jülich | |
| Kamps | Martina | Forschungszentrum Jülich | Jülich | |
| Kaus | Boris | JGU Mainz | Mainz | 5 |
| Körfgen | Bernd | Forschungszentrum Jülich | Jülich | |
| Kondov | Ivan | Karlsruhe Institute of Technology (KIT) | Eggenstein-Leopoldshafen | 51 |
| Korch | Matthias | University of Bayreuth | Bayreuth | 72 |
| Kostrzewa | Bartosz | Humboldt-Universität Berlin / DESY Zeuthen | Berlin | 60 |
| Kowalski | Piotr | Forschungszentrum Jülich | Jülich | 31 |
| Kremer | Kurt | MPI für Polymerforschung | Mainz | |
| Kremer | Manfred | Forschungszentrum Jülich | Jülich | |
| Krieg | Stefan | Forschungszentrum Jülich | Jülich | |
| Kropp | Thomas | Humboldt Universität zu Berlin | Berlin | 26 |
| Kuckuk | Sebastian | Universität Erlangen-Nürnberg | Erlangen | 73 |
| Kühne | Thomas | JGU Mainz | Mainz | |
| Kurzmann | André | Karlsruhe Institute of Technology | Karlsruhe | |
| Lähde | Timo | Forschungszentrum Jülich | Jülich | |
| Lechermann | Frank | University of Hamburg | Hamburg | 52 |
| Lehmann | Götz | HHU Düsseldorf | Düsseldorf | |
| Li | Jinyu | GRS | Jülich | 23 |
| Li | Yan | Forschungszentrum Jülich | Jülich | |
| Lippert | Thomas | Forschungszentrum Jülich | Jülich | |
| Liseykina | Tatyana | Universität Rostock | Rostock | 69 |
| Lücke | Monika | GRS | Aachen | 7 |
| Machtens | Jan-Philipp | Forschungszentrum Jülich | Jülich | 19 |
| Magiera | Martin | Universität Duisburg-Essen | Duisburg | 53 |
| Marenz | Martin | Universität Leipzig | Leipzig | 10, 11 |
| Mehrling | Timon | DESY | Hamburg | 70 |
| Meier | Patrick | TU Braunschweig | Braunschweig | 67 |
| Meinke | Jan | Forschungszentrum Jülich | Jülich | |
| Mellado | Juan Pedro | Max Planck Institute for Meteorology | Hamburg | 2 |

| Name | First Name | Affiliation | City | Poster No. |
|---|---|---|---|---|
| Michielsen | Kristel | Forschungszentrum Jülich | Jülich | |
| Mishra | Pankaj K. | DESY | Hamburg | 27 |
| Mnich | Joachim | DESY | Hamburg | |
| Mohlberg | Hartmut | Forschungszentrum Jülich | Jülich | |
| Mouhib | Halima | GRS | Aachen | |
| Müller | Marcus | Georg-August-Universität Göttingen | Göttingen | |
| Münster | Gernot | Universität Münster | Münster | |
| Müser | Martin | Forschungszentrum Jülich | Jülich | |
| Muñoz-Santiburcio | Daniel | Ruhr-Universität Bochum | Bochum | |
| Nadler | Walter | Forschungszentrum Jülich | Jülich | |
| Nuding | Win | Bergische Universität Wuppertal | Wuppertal | 54 |
| Öngüt | A. Emre | RWTH Aachen University | Aachen | 47 |
| Ohlmann | Sebastian | Universität Würzburg | Würzburg | 63, 64 |
| Orth | Boris | Forschungszentrum Jülich | Jülich | |
| Pagani | Giulia | Heinrich-Heine-University | Düsseldorf | 18 |
| Paul | Wolfgang | Martin Luther Universität | Halle | 13 |
| Peters | Norbert | RWTH Aachen University | Aachen | |
| Pfalzner | Susanne | Max-Planck-Institut für Radioastronomie | Bonn | 65 |
| Philipsen | Owe | University of Frankfurt | Frankfurt | |
| Poblete | Simón | Forschungszentrum Jülich | Jülich | 20 |
| Purnima | Sharma | Rhine Waal University of Applied Science | Kleve | |
| Rohlfs | Wilko | RWTH Aachen University | Aachen | 49 |
| Romero | Pedro A. | Fraunhofer-Institut für Werkstoffmechanik | Freiburg | 32 |
| Rushchanskii | Konstantin | Forschungszentrum Jülich | Jülich | 35 |
| Schaefer | Stefan | NIC, DESY | Zeuthen | |
| Schierholz | Gerrit | DESY | Hamburg | 61 |
| Schlößer | Tobias | Forschungszentrum Jülich | Jülich | |
| Schott | Benjamin | University of Leipzig | Leipzig | |
| Schroeder | Benjamin | Forschungszentrum Jülich | Jülich | |
| Schröer | Kevin | University of Duisburg-Essen | Duisburg | |
| Schuchart | Joseph | TU Dresden | Dresden | |
| Seino | Kaori | Uni Jena | Jena | 55 |
| Solar | Mathieu | Martin Luther Universität | Halle (Saale) | 9 |
| Sperling | Philipp | Universität Rostock | Rostock | 71 |
| Stengel | Holger | Universität Erlangen | Erlangen | 74 |
| Sukhomlinov | Sergey | Forschungszentrum Jülich | Jülich | |
| Szabo | Kalman | Forschungszentrum Jülich | Jülich | |
| Taslimi | Farzaneh | Forschungszentrum Jülich | Jülich | 14 |
| Tost | Holger | Johannes Gutenberg Universität Mainz | Mainz | 6 |
| Tóth | Bálint | Bergische Universität Wuppertal | Wuppertal | 62 |
| Treffon | Thorsten | Universität Stuttgart | Stuttgart | 59 |

| Name | First Name | Affiliation | City | Poster No. |
|---|---|---|---|---|
| Truhetz | Heimo | University of Graz | Graz | 3 |
| Vidossich | Pietro | GRS | Jülich | |
| Vincke | Kirsten | Max-Planck-Institut für Radioastronomie | Bonn | |
| von Domaros | Michael | University of Bonn | Bonn | 29 |
| von Mach | Christian | Forschungszentrum Jülich | Jülich | |
| Wittig | Hartmut | University of Mainz | Mainz | |
| Wolf | Dietrich | Universität Duisburg-Essen | Duisburg | |
| Zeller | Rudolf | Forschungszentrum Jülich | Jülich | |
| Zhang | Chao | Johannes Gutenberg University Mainz | Mainz | 15 |
| Zhang | Feichi | Karlsruhe Institute of Technology | Karlsruhe | 45 |
| Zhang | Jianguo | TU Darmstadt | Darmstadt | 24 |
| Zhou | Jiajia | University Mainz | Mainz | 46 |
| Zimmermann | Olav | Forschungszentrum Jülich | Jülich | 21 |